

Chemical Optimization of CBL0137 for Human African Trypanosomiasis Lead Drug Discovery

Baljinder Singh, Amrita Sharma, Naresh Gunaganti, Mitch Rivers, Pradip K. Gadekar, Brady Greene, Michael Chichioco, Carlos E. Sanz-Rodriguez, Courtney Fu, Catherine LeBlanc, Erin Burchfield, Nyle Sharif, Benjamin Hoffman, Gaurav Kumar, Andrei Purmal, Kojo Mensa-Wilmot,* and Michael P. Pollastri*

Cite This: *J. Med. Chem.* 2023, 66, 1972–1989

Read Online

ACCESS |



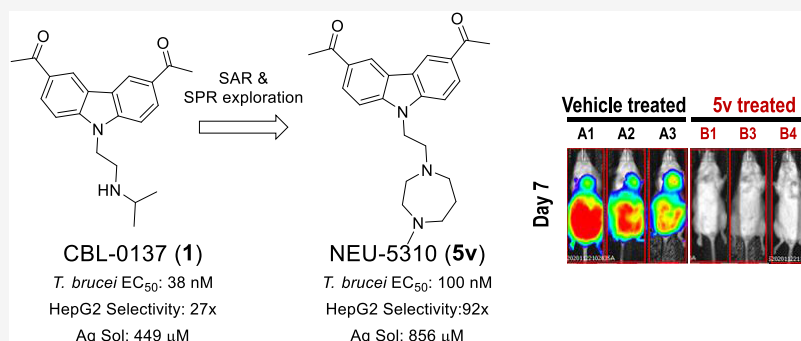
Metrics & More



Article Recommendations



Supporting Information



ABSTRACT: The carbazole CBL0137 (**1**) is a lead for drug development against human African trypanosomiasis (HAT), a disease caused by *Trypanosoma brucei*. To advance **1** as a candidate drug, we synthesized new analogs that were evaluated for the physicochemical properties, antitrypanosome potency, selectivity against human cells, metabolism in microsomes or hepatocytes, and efflux ratios. Structure–activity/property analyses of analogs revealed eight new compounds with higher or equivalent selectivity indices (**5j**, **5t**, **5v**, **5w**, **5y**, **8d**, **13i**, and **22e**). Based on the overall compound profiles, compounds **5v** and **5w** were selected for assessment in a mouse model of HAT; while **5v** demonstrated a lead-like profile for HAT drug development, **5w** showed a lack of efficacy. Lessons from these studies will inform further optimization of carbazoles for HAT and other indications.

INTRODUCTION

Human African trypanosomiasis (HAT) is caused by infection by the protozoan parasite *Trypanosoma brucei*. Endemic in 36 sub-Saharan African countries and transmitted by infected tsetse flies, HAT is considered fatal if untreated.¹ Due to poor financial incentives to pharmaceutical companies, the drug discovery efforts for neglected tropical diseases (NTDs) are not at a pace that matches the global burden of diseases.²

One approach to the discovery of new drugs for NTDs involves repurposing drugs developed for other diseases. Unlike direct repurposing, where an approved drug is utilized for a new indication, lead repurposing utilizes existing compounds as starting points for reoptimization. Using this approach, we identified a set of carbazole-derived compounds as hits for antitrypanosome drug discovery.³ The anticancer candidate CBL0137 (**1**), presently in human clinical trials,⁴ cured mice infected with trypanosomes.³ The properties and profile of **1** are listed in Table 1 alongside the preferred lead properties that we have employed in our drug discovery projects for HAT, noting that the desired physicochemical properties (cLogP, LogD, molecular weight, polar surface area)

are driven by their desirable ranges for CNS penetration and overall druglikeness.⁵ Herein, we report the structure–activity relationships (SARs) and structure–property relationships (SPRs) around the CBL0137 chemotype that led to the discovery of a new lead that is orally bioavailable.

RESULTS AND DISCUSSION

The primary goal of this study was to develop an understanding of SAR and SPR of chemotype **1**, with the aim of producing analogs with better metabolic, physicochemical, and trypanocidal properties than **1**. To accomplish this goal, four strategies were utilized (Figure 1). The first approach involved the modification of the amine region by exploring primary,

Received: October 31, 2022

Published: January 25, 2023



Table 1. Drug Parameter Thresholds and Corresponding Values of CBL0137 (1)

	desired	CBL0137 (1)
<i>T. brucei</i> EC ₅₀ (μM)	≤0.20	0.038
selectivity index vs HepG2 cells	≥25	27
cLogP	≤3	2.8
polar surface area (Å ²)	40 < x < 90	51
lipophilic ligand efficiency (LLE) ^a	≥4	4.6
thermodynamic aqueous solubility (μM)	≥100	449
molecular weight (g/mol)	≤450	336
Log D _{7.4}	≤2	2.1
human liver microsome (HLM) CL _{int} (μL/min/mg protein)	<8.6	7.1
rat hepatocyte CL _{int} (μL/min/10 ⁶ cells)	<5.1	37

^aLipophilic ligand efficiency (LLE) = pEC₅₀ - clogP.

secondary, and diamines and by replacing the exocyclic N-atom with other heteroatoms. In the second approach, the acetyl groups were altered by heterocyclic and bioisosteric replacements. In the third strategy, crossover compounds were synthesized by selecting a combination of the best features identified in approaches 1 and 2. Additionally, in the fourth strategy, compound 1 was truncated to identify a minimal pharmacophore with antitrypanosome activity.

Amine Replacements. Compounds 5a–y were synthesized as described in Schemes 1–3, a variation of methods previously described.⁶ The acetylated carbazole-3 was produced via the Friedel–Crafts acylation of carbazole 2. Compound 3 was then reacted with either 1,2-dibromoethane or tosylated bromoethanol to produce intermediate 4, which was then reacted with a variety of amines for the final compounds 5a–ab (Scheme 1 and Tables 2–4). Analogs 5ac–al were synthesized via reductive amination of the aldehyde intermediate 7 (Scheme 2), which was prepared by the reaction of 3 with bromoethanol. Compound 9 was synthesized by the alkylation of intermediate 3 (Scheme 3).

Initially, the isopropylamine of 1 was replaced with a variety of primary and secondary amines. Replacement with primary aminocarbocycles (5a–e) ranging in size from cyclopropyl to cycloheptyl showed good potency against *T. brucei* but failed to improve the selectivity index (SI) compared to 1. Matched pair analysis showed that tertiary amines had better selectivity indices than secondary amines (5h, SI > 4167 vs 5b, SI = 3.5; 5j, SI = 97 vs 5d, SI = 22; Table 2). A compound bearing an azetidine ring (5h) was the most potent from this series with EC₅₀ < 0.006 μM (SI > 4167). SAR was further explored around the azetidine replacement with different substitutions.

Substitution on the azetidine ring (5k–m) reduced antitrypanosome potency (Table 2).

N-Methylated analogs of 1 (see 5ac) and 5w (see 5ae) were prepared to identify the importance of the H-bond donor on the isopropylamine functionality. Results varied widely from EC₅₀ of 0.025 μM for 5ac to EC₅₀ = 0.28 μM for 5ae (Tables 2 and 3), implying that the H-bond donor was not essential for antitrypanosome potency.

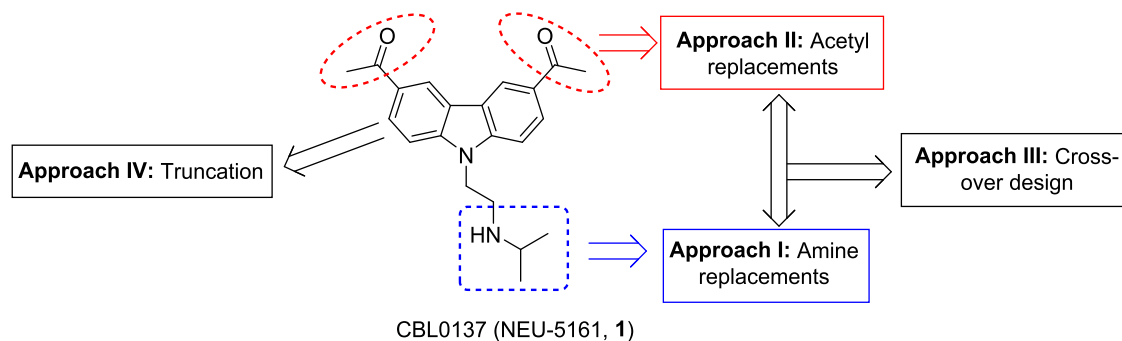
Diamine analogs were prepared next (5s–z and 5ae–ak; Table 3). Compounds 5v, 5w, and 5af were the most potent (EC₅₀ ≤ 0.1 μM), with good selectivity (SI > 100) and good ADME properties (Table 3). Lipophilic ligand efficiency (LLE = pEC₅₀ - cLogP), with a desirable LLE ≥ 4,⁷ describes the quality of a compound by normalizing that compound's potency against (mere) lipophilicity. As observed with 1 (LLE = 4.6), 5w, 5h, and 5v had excellent LLE values of 6.0, >5.9, and 4.7, respectively (Tables 2 and 3).

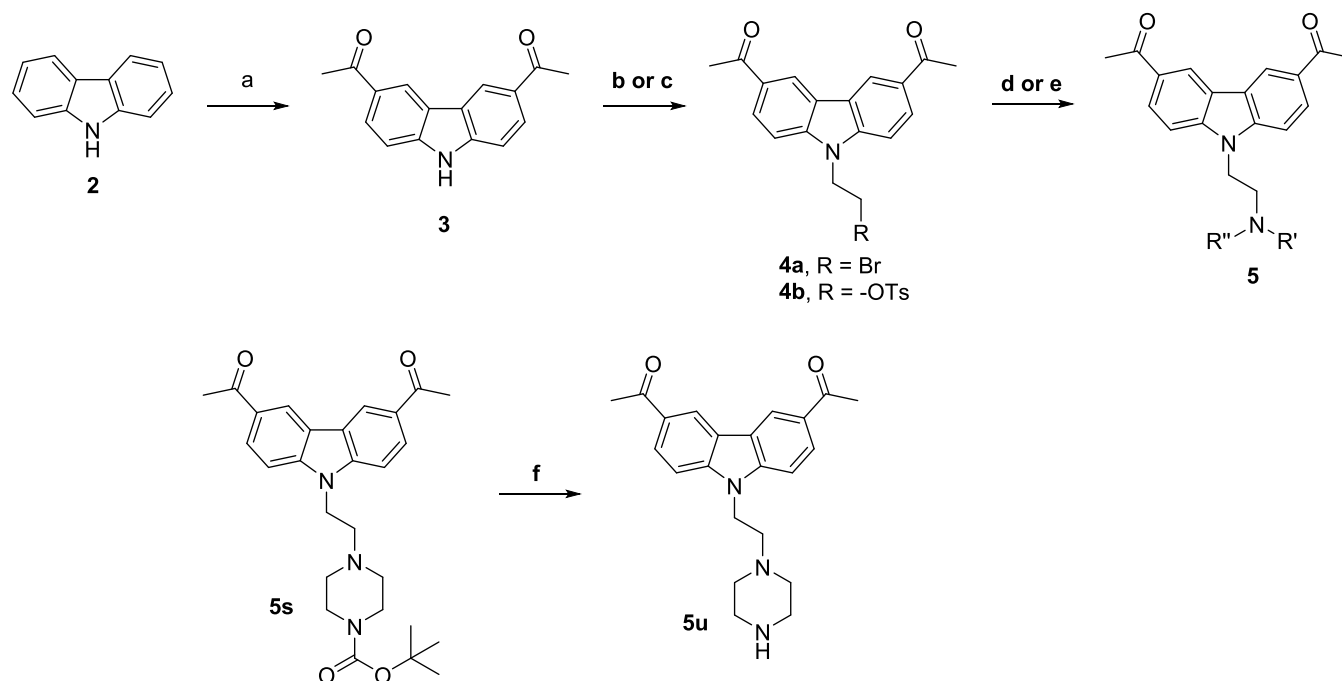
Replacement of the isopropylamine of 1 with ring systems (5a–e; 5h–r) reduced potency against *T. brucei*. Substitution with a spirocyclic moiety (5al) reduced potency and increased hepatocyte clearance. Finally, when the nitrogen atom of the isopropylamine was replaced with oxygen (9) or sulfur atoms (5z), a 100-fold loss in antitrypanosome activity occurred (Table 4).

Acetyl Replacements. Compounds 12, 15, 21, and 22 were synthesized, as shown in Schemes 4–7. The first set of compounds were the replacement of acetyl with heterocycles, obtained via intermediate 10, produced from dibromocarbazole (9). Palladium-mediated coupling was then performed on intermediate 11 to yield the final compounds 12.

Other replacements for the acetyl moieties were explored; acetamide (12h –7393), amine (12j), nitrile (15), ethyl ester (21a), trifluoromethyl (21b), trifluoromethoxy (21c –6877), and oxime (22) analogs were prepared as described in Schemes 5–7. Compound (15) was prepared via cyanation of dibromocarbazole (9) followed by installation of the amine functionality via displacement (Scheme 5), as described in Scheme 1. Compounds 21 were prepared via palladium-mediated coupling of an aryl halide and aniline to yield compounds 18, followed by ring closing to obtain 19. Conversion to the final compounds 21 (Scheme 6) was readily achieved by amine displacement. Compound 22 was prepared from 1 by reacting it with methoxyamine (Scheme 7).

Replacement of the acetyl groups with various heterocycles resulted in compounds with desired potency but poor aqueous solubility, with the exception of 12a (solubility = 537 μM). However, microsomal clearance was high for 12a. We conclude

**Figure 1.** Structure of 1 and synthesis strategies employed.

Scheme 1. Synthetic Route for Compounds 5a–ab^a

^aReagents and conditions: (a) acetyl chloride, AlCl₃, dichloromethane, 0 °C to room temperature (rt), 48 h; (b) dibromoethane, NaH, dimethylformamide (DMF), 60 °C, 40 min; (c) 2-bromoethyl 4-methylbenzenesulfonate, Cs₂CO₃, DMF, rt, 16 h; (d) amine, *iso*-propyl alcohol (IPA), microwave 100 °C, 30–90 min; (e) amine, DMF, microwave 100 °C, 30 min; and (f) trifluoroacetic acid (TFA), dichloromethane, rt, 1 h.

that the replacement of the acetyl groups on **1** with heterocycles is not a productive strategy for our purposes. While many of acetyl replacements boosted activity, this was accompanied by an undesirable reduction of aqueous solubility (Table 5). Notably, the trifluoromethyl and trifluoromethoxy analogs (**21b–c**) were exceptions to this trend.

Crossover Design. “Crossover” compounds (**21e–f**; Table 6) were designed to enhance the aqueous solubility of **21b** and **21c** (Table 5) by incorporating an *N,N*-dimethylethylenediamine tail from **5w**. The crossover compounds had higher solubility and potency. In a comparison of matched pairs, the aqueous solubility of **21e** increased by 500-fold to 384 μM compared to 0.7 μM for **21e** while retaining the excellent antitrypanosome potency. In the case of **21f**, aqueous solubility showed a modest increase (to 53 μM), compared to that of the parent **21c**, which had an aqueous solubility of 34 μM.

Compound Truncation. Compound **1** was truncated to identify a minimum pharmacophore with antitrypanosome activity. Elimination of one acetyl group reduced the potency by 22-fold (**21g**) but increased the aqueous solubility by 2-fold compared to **1**. Removal of the pendant amine group (**3**) eliminated the antitrypanosome activity and increased the metabolic clearance compared to that of **1**. Conversion of the carbazole core to an indole (**25**, prepared as shown in Scheme 8) led to the loss of activity (Table 7). Highlights of the SAR and SPR identified are summarized in Figure 2.

Cell Permeability, Metabolism, and Safety Profiling of Hits. Based on the antitrypanosome potency and physicochemical properties, five compounds were selected for Caco-2 permeability measurement, mouse plasma stability, mouse liver microsome clearance, and cytochrome P450 inhibition. All compounds were stable in mouse plasma and liver microsomes. No cytochrome P450 liability was observed at 10 μM. Compounds **5h**, **5v**, and **5w** had acceptable

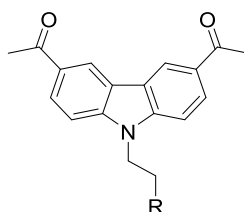
permeability and efflux ratio in Caco-2 cells, whereas compounds **5af** and **21e** were rapidly effluxed (defined as an efflux ratio >2.0; Table 8).

As shown in Tables 8 and 9, compounds **5w** and **5v** are promising compounds for advancement to the next set of assays and potentially to *in vivo* studies. We selected **5v** on the basis of its longer half-life in mouse plasma, its higher aqueous solubility, and its marginally lower efflux ratio.

Trypanocidal of 5v and 5w. As a metric for the irreversible killing of trypanosomes, the cidality of **5v** was determined after a short-term (6 h) exposure of cells to the hit.⁸ The concentration of **5v** that caused 50% trypanocidal (DCC₅₀) was 160 nM, and 90% cidality (DCC₉₀) required 870 nM of the compound (Figure 3). For **5w**, DCC₅₀ and DCC₉₀ were 690 nM and 5.6 μM, respectively. We conclude that **5v** is 6-fold more trypanocidal than **5w** based on the ratio of DCC₉₀'s.

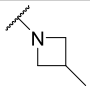
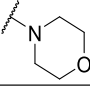
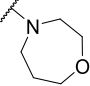
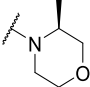
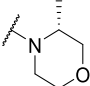
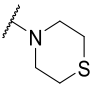
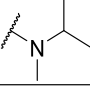
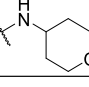
Pharmacokinetics (PK) and Efficacy of 5v and 5w in a Mouse Model of HAT. Based upon the overall *in vitro* potency, physicochemical properties, and cell permeability, we advanced **5v** and **5w** as “proof of principle” in efficacy studies in a mouse model of HAT. First, we measured a repeated maximum tolerated dose (rMTD) for each compound. Swiss-Webster mice (male and female; 8–9 weeks old) were administered compounds at 30, 60, or 120 mg/kg daily (orally) for a total of 10 days. Mice were monitored daily for overall conditions based upon the parameters described in Table S2 (see the Supporting Information) as well as changes in body weight up to 7 days post administration of the drug. Dosing of **5v** or **5w** at 30, 60, or 120 mg/kg to male and female mice did not significantly affect the overall condition of the mice or cause significant weight loss. Thus, the rMTD of both compounds is above 120 mg/kg.

Table 2. Amine Replacement Analogues (Approach I): Potency, Selectivity Index (SI), and Physicochemical and Metabolic Properties



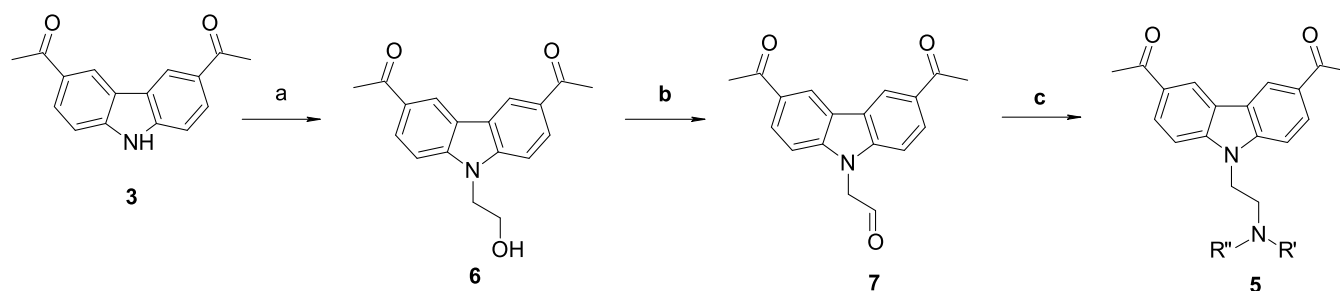
Entry	R	<i>T. brucei</i> EC ₅₀ , μM ± SD (Selectivity index ^a)	<i>T. brucei</i> LLE ^b	Aq. sol. (μM)	Human Liver Microsome CL _{int} (μL/min/mg protein)	Rat hepatocyte CL _{int} (μL/min/10 ⁶ cells)
1		0.037 (27)	4.6	449	7.1	37
5a		0.27±0.05 (31)	4.0	37	65	111
5b		0.046±0.016 (3.5)	4.4	180	34	74
5c		0.021±0.014 (nd)	4.3	252	40	71
5d		0.030±0.014 (22)	3.7	81	66	106
5e		0.032±0.001 (9.8)	3.2	17	184	132
5f		0.046±0.012 (nd)	4.4	196	26	68
5g		0.41±0.209 (66)	3.4	0.90	65	138
5h		<0.006 (>4000)	>5.9	655	8.0	8.3
5i		0.13±0.01 (45)	4.0	450	8.9	59
5j		0.032±0.005 (97)	4.2	133	54	157
5k		1.5±0.109 (11)	3.29	105	54.1	35.5
5l		1.2±0.456 (26)	2.94	10	35.5	115

Table 2. continued

Entry	R	<i>T. brucei</i> EC ₅₀ , μM ± SD (Selectivity index ^a)	<i>T. brucei</i> LLE ^b	Aq. sol. (μM)	Human Liver Microsome CL _{int} (μL/min/mg protein)	Rat hepatocyte CL _{int} (μL/min/10 ⁶ cells)
5m		0.13±0.007 (22)	4.09	661	28.6	46.5
5n		0.18±0.1 (133)	4.5	23	26	141
5o		0.23±0.03 (26)	4.35	174	63	291
5p		0.19±0.08 (25)	4.08	26	62	>300
5q		0.42±0.09 (26)	3.73	16	106	217
5r		1.1±0.169 (10)	3.15	4.0	>300	>300
5ac		0.025±0.004 (19)	4.38	>1000	26	50
5ad		0.13±0.01 (31)	4.87	118	21	27

^aSelectivity index = HepG2 TC₅₀/*T. brucei* EC₅₀; “nd” indicates “not determined”. ^bLipophilic ligand efficiency (LLE) = pEC₅₀ – clogP; additional ADME data, including Log D_{7.4} and human plasma protein binding, are included in Table S1 of the Supporting Information.

Scheme 2. Synthetic Route for Compounds 5ac–al^a

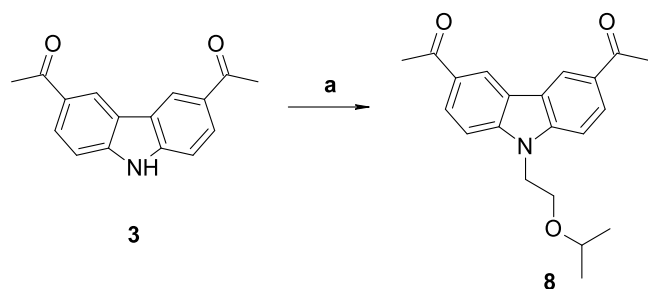


^aReagents and conditions: (a) 2-bromoethanol, Cs₂CO₃, DMF, 60 °C, 16 h; (b) Dess–Martin periodinane, acetonitrile (ACN), 80 °C, 80 min; and (c) amine, acetic acid, sodium triacetoxyborohydride, dichloroethane, molecular sieves, rt, 2.5 h.

Pharmacokinetics (PK) parameters of **5v** were determined in the plasma of female Swiss-Webster mice dosed orally with 80 mg/kg (70% of rMTD). The peripheral blood level of **5v** over time is shown in Figure S1. The C_{max} of **5v** was 5680 ng/mL (**5v** EC₅₀ corrected for the observed 55% protein binding = 356 ng/mL) (Table S3). The average concentration of **5v** for 4 h was 6.8 μM, which is above the desired plasma level of more than 10× EC₅₀ for at least 4 h. Similarly, the PK parameters of **5w** were also determined with an 80 mg/kg oral dose, and blood levels are shown in Figure S1. The C_{max} of **5w** was 11636 ng/mL (**5w** EC₅₀ corrected for the observed 44% protein binding = 6.9 ng/mL) (Table S3). The average concentration of **5w** for 4 h was 17.9 μM, which is above the desired plasma

level of more than 10× EC₅₀ for at least 4 h. Other PK parameters of **5v** and **5w** are summarized in the Supporting Information (Table S3).

Based on the promising PK, antiproliferative potency, trypanocidal, metabolism, and physicochemical properties, we tested both compounds in a mouse model of HAT. Since the majority of HAT cases manifest as a chronic infection, we tested the efficacy with pleomorphic *T. brucei* AnTat1.1, whose course of disease parallels a chronic infection with the parasite.⁹ With **5v**-treated mice, a 58-fold reduction in trypanosome tissue load, monitored by the bioluminescence signal, was observed on day 4 (Figure 4).^{10,11} On day 7, tissue parasite load decreased by 165-fold, qualifying **5v** as a “lead”

Scheme 3. Synthetic Route for Compounds 9^a

^aReagents and conditions: (a) 2-(2-bromoethoxy)propane, Cs₂CO₃, DMF, rt, 16 h.

for HAT drug development. Conversely, despite the high potency and exposure of **5w**, there was no meaningful difference in infection levels as compared to the controls; this is likely due to the inferior cidalty observed versus **5v**.

CONCLUSIONS

With the aim of finding new compounds with improved potency, selectivity, and physicochemical properties compared to **1**, a systematic medicinal chemistry approach was used to generate new carbazoles that were tested for selectivity in the inhibition of *T. brucei* proliferation and trypanocidal activity, as well as the physicochemical and ADME properties. This work led to the identification of **5v**, which in a mouse model of chronic HAT reduced the trypanosome tissue load by 165-fold. Work is ongoing to identify a dosing regimen of **5v** that can cure a chronic HAT infection in mice. Other compounds in our collection (Table 9) will be evaluated to find out whether any others, like **5v**, may be leads for antitrypanosome drug discovery based on their overall profiles.

EXPERIMENTAL SECTION

General Chemistry. All reagents and starting materials were procured commercially from Sigma-Aldrich Inc., Fisher Scientific, or Combi-blocks and used as received. Melting points were recorded on a Thermo Scientific MEL-TEMP apparatus. NMR spectra were obtained on a Varian NMR system operating at 400 and 500 MHz. Chemical data for protons are reported in parts per million (ppm) downfield from tetramethylsilane and are referenced to the residual proton in the NMR solvent [(CD₃)₂SO, 2.50; CD₃OD, 3.31; CDCl₃, 7.26; (CD₃)₂CO, 2.05; ppm]. Liquid chromatography-mass spectrometry (LCMS) analysis was performed using a Waters e2795 Alliance or Waters e2695 Alliance or Agilent 1100 reverse-phase high-performance liquid chromatography-mass spectrometry (HPLC-MS) and a 3.5 μm Waters SunFire C18 4.6 × 50 mm column, with a multiwavelength photodiode array detector (λ = 200–600 nm) and a MicroMass ZQ single quadrupole mass spectrometer (electrospray ionization). Gradients for the LCMS analysis were water or acetonitrile, both with 0.1% v/v of formic acid (method A: 5% acetonitrile to 100% acetonitrile for 0–4 min; method B: 5% acetonitrile to 100% acetonitrile for 0–8 min; method C: 0% acetonitrile to 50% acetonitrile for 0–4 min). Microwave reactions were performed in a Biotage Initiator+ or CEM Discovery SP instrument. Purification of intermediates and final compounds was performed using silica gel chromatography using the Biotage IsoleraOne flash purification system or unless otherwise noted. All newly synthesized compounds were deemed >95% pure by LCMS (PDA, λ = 200–600 nm).

Chemistry Experiments. *Synthesis of 1,1'-(9H-Carbazole-3,6-diyl)bis(ethan-1-one) (3).* 9H-Carbazole (**2**, 6.00 g, 35.9 mmol) was taken up in dichloromethane (90 mL) under stirring at room temperature, giving a yellow suspension. The temperature was

lowered to 0 °C, and aluminum chloride (14.1 g, 78.9 mmol) was added portionwise, giving an orange suspension. Acetyl chloride (12.8 mL, 179.4 mmol) was then added dropwise over a period of 5 min. The reaction was left stirring in an ice bath and allowed to warm to room temperature under stirring over a period of 2 days. The reaction was then lowered to 0 °C and quenched with saturated sodium bicarbonate under stirring (200 mL). The reaction vessel was then allowed to warm to room temperature under stirring for 20 min. At this time, the reaction was extracted from ethyl acetate (5 × 300 mL). The combined organic layers were dried over magnesium sulfate, filtered, and evaporated to dryness. The crude material was then stirred in 20% ethyl acetate/hexanes (120 mL) for 30 min at room temperature. The solid was collected by vacuum filtration, washed with 20% ethyl acetate/hexanes, and dried to afford a light brown powder of 1,1'-(9H-carbazole-3,6-diyl)bis(ethan-1-one) (**6.17 g**, 68%). ¹H NMR (500 MHz, DMSO-*d*₆) δ ppm 12.08 (s, 1H) 9.04 (s, 2H) 8.07 (dd, *J* = 8.5, 1.7 Hz, 2H) 7.61 (d, *J* = 8.8 Hz, 2H) 2.70 (s, 6H). LCMS: 251 [M + H]⁺.

Synthesis of 1,1'-(9-(2-Bromoethyl)-9H-carbazole-3,6-diyl)bis(ethan-1-one) (4a). 1,1'-(9H-Carbazole-3,6-diyl)bis(ethan-1-one) (**3**, 100 mg, 398 μmol) was dissolved in *N,N*-dimethylformamide (1.5 mL) and heated to 60 °C. Sodium hydride (127.33 mg, 3.18 mmol) was then added, and the mixture was allowed to stir for 30 min. Dibromoethane (2.99 g, 15.9 mmol) was then added. The reaction mixture was left stirring at 60 °C for 40 min. The mixture was diluted with water, extracted 3× with ethyl acetate, washed with water and brine, and then dried with magnesium sulfate. The crude material was purified by silica gel chromatography (30% ethyl acetate/cyclohexane) to afford 1,1'-(9-(2-bromoethyl)-9H-carbazole-3,6-diyl)bis(ethan-1-one) as a white powder (68.4 mg, 48.0%). ¹H NMR (400 MHz, DMSO-*d*₆): δ 9.07 (s, 2 H), 8.13 (d, *J* = 8.61 Hz, 2 H), 7.84 (d, *J* = 8.61 Hz, 2 H), 4.98 (t, *J* = 5.86 Hz, 2 H), 3.98 (t, *J* = 5.86 Hz, 2 H), 2.71 (s, 6 H). LCMS: 358 (Br⁷⁹), 360 (Br⁸¹) [M + H]⁺.

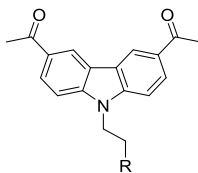
Synthesis of 2-(3,6-Diacetyl-9H-carbazol-9-yl)ethyl 4-Methylbenzenesulfonate (4b). 1,1'-(9H-Carbazole-3,6-diyl)bis(ethan-1-one) (**2**, 615 mg, 2.45 mmol), 2-bromoethyl-4-methylbenzenesulfonate (2.05 g, 7.34 mmol), and cesium carbonate (2.39 g, 7.34 mmol) were taken up in *N,N*-dimethylformamide (36 mL) under stirring at room temperature for 3 days. The reaction was diluted with water (300 mL) and extracted from ethyl acetate (5 × 100 mL). The combined organic layers were washed with a saturated brine solution. Following this, the combined organic layers were dried over sodium sulfate, filtered, and evaporated to dryness, affording a crude yellow solid. The crude material was purified via silica gel chromatography (0–100% ethyl acetate/hexane) to afford a yellow amorphous solid of 2-(3,6-diacetyl-9H-carbazol-9-yl)ethyl 4-methylbenzenesulfonate (645 mg, 58%). ¹H NMR (500 MHz, CDCl₃) δ 8.74 (d, *J* = 0.98 Hz, 2 H), 8.14 (dd, *J* = 8.78, 1.46 Hz, 2 H), 7.37 (d, *J* = 8.78 Hz, 2 H), 7.24 (d, *J* = 8.30 Hz, 2 H), 6.87 (d, *J* = 7.81 Hz, 2 H), 4.59–4.66 (m, 2 H), 4.47 (t, *J* = 5.37 Hz, 2 H), 2.77 (s, 6 H), 2.26 (s, 3 H). LCMS: 450.1 [M + H]⁺.

General Method for Preparation of Compounds 5a–ab. Compound **4a** or **4b** was dissolved in either IPA or DMF (0.1 M). To this, desired amines (5–10 equiv) were added and the reaction was heated in a microwave at 100 °C for 30–90 min. On completion, the reaction mixture was then partitioned thrice with water and ethyl acetate. The organic layer was dried and then purified by flash chromatography using 0–50% of methanol in dichloromethane gradient to get the desired product.

1,1'-(9-(2-(Cyclopropylamino)ethyl)-9H-carbazole-3,6-diyl)bis(ethan-1-one) (5a). (Yield: 35%): ¹H NMR (500 MHz, CDCl₃) δ 0.33 (brs, 2H), 0.43–0.48 (m, 2H), 2.12–2.17 (m, 1H), 2.76 (s, 6H), 3.22 (t, *J* = 6.59 Hz, 2H), 4.50 (t, *J* = 6.59 Hz, 2H), 7.53 (d, *J* = 8.78 Hz, 2H), 8.19 (d, *J* = 8.30 Hz, 2 H), 8.80 (s, 2H). LCMS found 335.14 [M + H]⁺.

1,1'-(9-(2-(Cyclobutylamino)ethyl)-9H-carbazole-3,6-diyl)bis(ethan-1-one) (5b). (Yield: 37%): ¹H NMR (500 MHz, CDCl₃) δ 1.55–1.69 (m, 4 H), 2.11–2.23 (m, 2 H), 2.75 (s, 6 H), 3.05 (t, *J* = 6.59 Hz, 2 H), 3.24–3.33 (m, 1 H), 4.48 (t, *J* = 6.59 Hz, 2 H), 7.53

Table 3. Diamine Analogues (Approach I): Potency, Selectivity Index, and Physicochemical and Metabolic Properties



Entry	R	<i>T. brucei</i> EC ₅₀ (μM) (Selectivity index ^a)	<i>T. brucei</i> LLE ^b	Aq. sol. (μM)	Human Liver Microsome CL _{int} (μL/min/mg protein)	Rat hepatocyte CL _{int} (μL/min/10 ⁶ cells)
5s		1.2±0.36 (>33)	2.7	1.0	>300	194
5t		0.35±0.003 (40)	4.2	848	8.5	22
5u		0.35±0.08 (20)	4.5	533	7.9	14
5v		0.10±0.01 (92)	4.7	856	16	26
5w		0.0083±0.006 (662)	6.0	667	7.9	6.7
5x		0.12±0.073 (nd)	4.8	516	>300	2.8
5y		0.57±0.023 (47)	3.9	711	28	8.2
5ae		0.28±0.054 (7.1)	4.1	680	17	32
5af		0.074±0.04 (36)	3.9	819	<3.0	2.4
5ag		0.17±0.11 (35)	4.3	568	83	20
5ah		0.40±0.09 (17)	4.3	818	<3.0	8.3
5ai		0.62±0.026 (nd)	3.5	47	75	33
5aj		0.65±0.12 (nd)	4.1	--	--	--
5ak		0.26±0.036 (41)	4.1	>1000	217	37

^aSelectivity index = HepG2 TC₅₀/*T. brucei* EC₅₀; nd indicates not determined. ^bLipophilic ligand efficiency (LLE) = pEC₅₀ - clogP; additional ADME data, including Log D_{7.4} and human plasma protein binding, are included in Table S1 of the Supporting Information.

(d, *J* = 8.78 Hz, 2 H), 8.19 (dd, *J* = 8.78, 1.46 Hz, 2 H), 8.80 (d, *J* = 1.46 Hz, 2 H). LCMS found 349.17 [M + H]⁺.

1,1'-(9-(2-(Cyclopentylamino)ethyl)-9H-carbazole-3,6-diyl)bis(ethan-1-one) (5c). (Yield: 46%): ¹H NMR (500 MHz, CDCl₃) δ 1.21–1.27 (m, 3 H), 1.46–1.53 (m, 2 H), 1.59–1.65 (m, 2 H), 1.75–1.83 (m, 2 H), 2.73 (s, 6 H), 3.05–3.08 (m, 1 H), 3.08–3.12 (m, 2 H), 4.48 (t, *J* = 6.59 Hz, 2 H), 7.52 (d, *J* = 8.30 Hz, 2 H), 8.14–8.18 (m, 2 H), 8.77 (s, 2 H). LCMS found 363.17 [M + H]⁺.

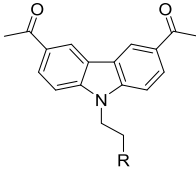
1,1'-(9-(2-(Cyclohexylamino)ethyl)-9H-carbazole-3,6-diyl)bis(ethan-1-one) (5d). (Yield: 55%): ¹H NMR (500 MHz, CDCl₃) δ 1.00 (d, *J* = 12.69 Hz, 2 H), 1.09–1.28 (m, 4 H), 1.65–1.72 (m, 2 H), 1.80 (d, *J* = 10.74 Hz, 2 H), 2.38–2.45 (m, 1 H), 2.75 (s, 6 H), 3.14 (t, *J* = 6.59 Hz, 2 H), 4.48 (t, *J* = 6.59 Hz, 2 H), 7.53 (d, *J* = 8.78 Hz,

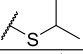
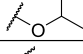
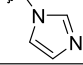
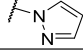

2 H), 8.18 (dd, *J* = 8.78, 1.46 Hz, 2 H), 8.79 (s, 2 H). LCMS found 377.17 [M + H]⁺.

1,1'-(9-(2-(Cycloheptylamino)ethyl)-9H-carbazole-3,6-diyl)bis(ethan-1-one) (5e). (Yield: 65%): ¹H NMR (500 MHz, CDCl₃) δ 1.25–1.37 (m, 4 H), 1.41–1.62 (m, 6 H), 1.70–1.76 (m, 2 H), 2.57–2.65 (m, 1 H), 2.75 (s, 6 H), 3.10 (t, *J* = 6.59 Hz, 2 H), 4.47 (t, *J* = 6.59 Hz, 2 H), 7.53 (d, *J* = 8.78 Hz, 2 H), 8.18 (dd, *J* = 8.78, 1.46 Hz, 2 H), 8.79 (d, *J* = 1.46 Hz, 2 H). LCMS found 391.21 [M + H]⁺.

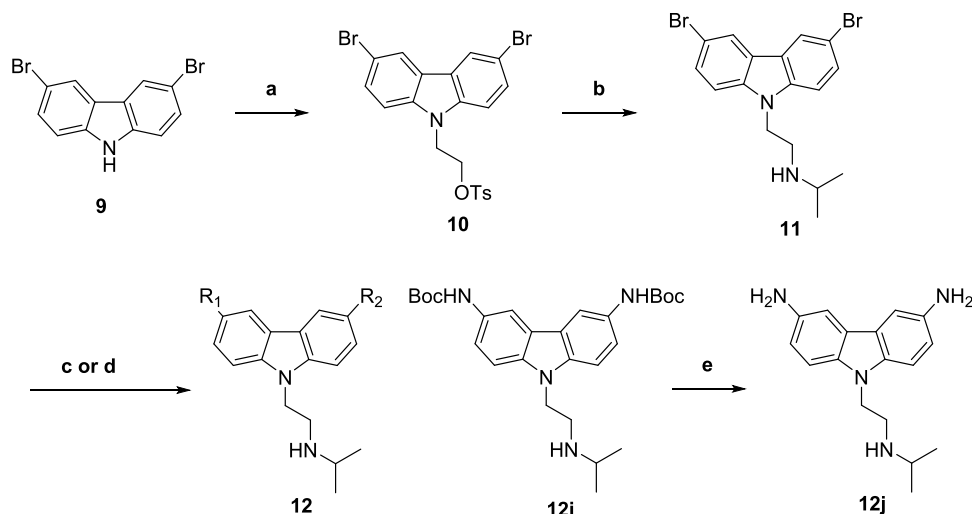
1,1'-(9-(2-(Propylamino)ethyl)-9H-carbazole-3,6-diyl)bis(ethan-1-one) (5f). (Yield: 44%): ¹H NMR (500 MHz, CDCl₃) δ 0.86 (t, *J* = 7.41 Hz, 3 H), 1.39–1.50 (m, 2 H), 2.60 (t, *J* = 7.41 Hz, 2 H), 2.76 (s, 6 H), 3.14 (t, *J* = 6.59 Hz, 2 H), 4.52 (t, *J* = 6.31 Hz, 2 H), 7.55 (d, *J* = 8.78 Hz, 2 H), 8.19 (dd, *J* = 8.78, 1.65 Hz, 2 H), 8.80 (d, *J* = 1.10 Hz, 2 H). LCMS found 337.10 [M + H]⁺.

Table 4. Amine Replacement Analogues (Approach I): Potency, Selectivity Index, and Physicochemical and Metabolic Properties



Entry	R	<i>T. brucei</i> EC ₅₀ (μM) / (Selectivity index) ^a	<i>T. brucei</i> LLE ^b	Aq. sol. (μM)	Human Liver Microsome CL _{int} (μL/min/mg protein)	Rat hepatocyte CL _{int} (μL/min/10 ⁶ cells)
5z		4.4±0.72 (>6.4)	1.6	2.0	88	>300
8		3.7±0.36 (8.1)	2.3	7.0	63	>300
5aa		3.6±0.584 (>8.1)	3.1	11	20	24
5ab		7.0±1.91 (>4.1)	2.5	13	25	97
5al		0.45±0.14 (nd)	4.4	157	18	>300

^aSelectivity index = HepG2 TC₅₀/*T. brucei* EC₅₀; nd indicates not determined. ^bLipophilic ligand efficiency (LLE) = pEC₅₀ – clogP; additional ADME data, including Log D_{7.4} and human plasma protein binding, are included in Table S1 of the Supporting Information.

Scheme 4. Synthetic Route for Compounds 12^a

^aReagents and conditions: (a) 2-bromoethyl 4-methylbenzenesulfonate, Cs₂CO₃, DMF, rt, 16 h; (b) isopropylamine, DMF, microwave 100 °C, 30 min; (c) boronic acid/ester, Pd₂dba₃, PCy₃, K₂CO₃, DMF/water (3:1), microwave, 130 °C, 3 h; (d) amine, Pd₂dba₃, *t*-BuXPhos, potassium 2-methylpropan-2-olate, dioxane, microwave, 110 °C, 35 min; and (e) 4.0 M HCl in dioxane, rt.

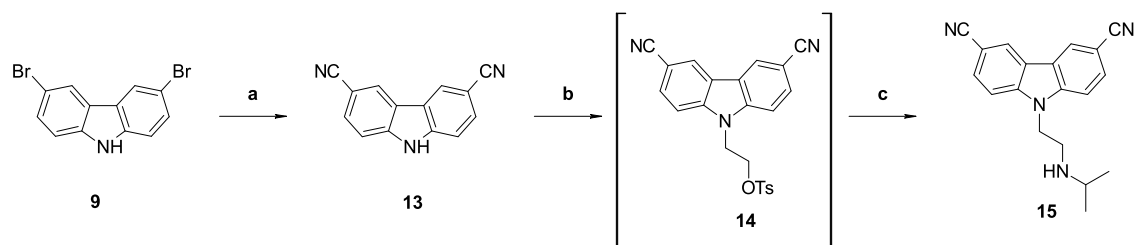
1,1'-(9-(2-((2,2,2-Trifluoroethyl)amino)ethyl)-9H-carbazole-3,6-diyl)bis(ethan-1-one) (**5g**). (Yield: 10%): ¹H NMR (500 MHz, CDCl₃) δ 2.76 (s, 6 H), 3.15 (d, *J* = 9.33 Hz, 2 H), 3.28 (t, *J* = 5.49 Hz, 2 H), 4.51 (t, *J* = 6.31 Hz, 2 H), 7.53 (d, *J* = 8.78 Hz, 2 H), 8.20 (dd, *J* = 8.51, 1.37 Hz, 2 H), 8.81 (d, *J* = 1.10 Hz, 2 H). LCMS found 377.20 [M + H]⁺.

1,1'-(9-(2-(Azetidin-1-yl)ethyl)-9H-carbazole-3,6-diyl)bis(ethan-1-one) (**5h**). (Yield: 18%): ¹H NMR (400 MHz, CD₃OD) δ 2.05 (t, *J* = 7.05 Hz, 2 H), 2.75 (s, 6 H), 3.02 (t, *J* = 6.14 Hz, 2 H), 3.23 (t, *J* = 7.33 Hz, 4 H), 4.47 (t, *J* = 6.32 Hz, 2 H), 7.68 (d, *J* = 8.79 Hz, 2 H), 8.22 (d, *J* = 8.61 Hz, 2 H), 8.93 (s, 2 H): LCMS found 335.21 [M + H]⁺.

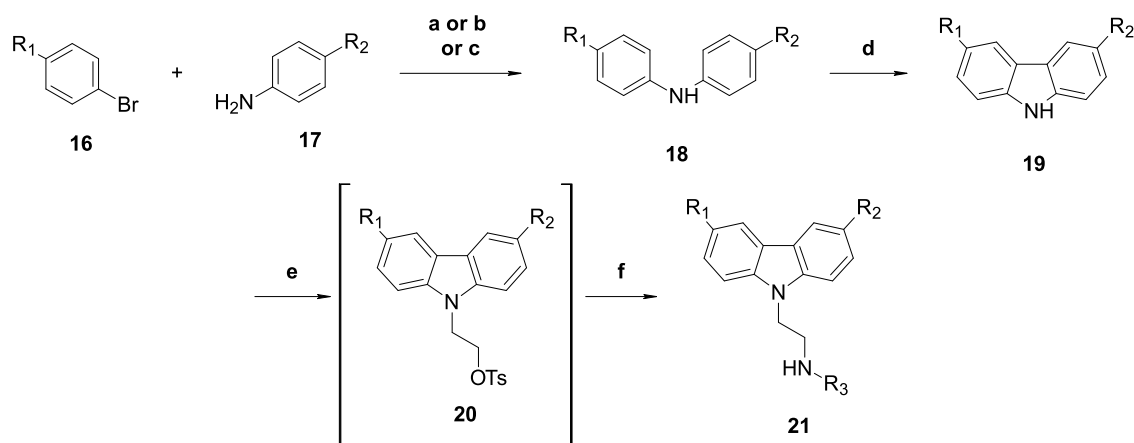
1,1'-(9-(2-(Pyrrolidin-1-yl)ethyl)-9H-carbazole-3,6-diyl)bis(ethan-1-one) (**5i**). (Yield: 24.2%): ¹H NMR (400 MHz, CD₃OD) δ 1.81 (brs, 4 H), 2.64 (brs, 4 H), 2.69–2.74 (m, 6 H), 2.93 (t, *J* = 7.14 Hz, 2 H), 4.53 (t, *J* = 7.24 Hz, 2 H), 7.58–7.63 (m, 2 H), 8.17 (d, *J* = 8.61 Hz, 2 H), 8.85 (s, 2 H). LCMS found 349.24 [M + H]⁺.

1,1'-(9-(2-(Piperidin-1-yl)ethyl)-9H-carbazole-3,6-diyl)bis(ethan-1-one) (**5j**). (Yield: 26%): ¹H NMR (500 MHz, CDCl₃) δ 1.41–1.49 (m, 6 H), 2.50 (br. s., 4 H), 2.76 (s, 8 H), 4.47–4.53 (m, 2 H), 7.51 (d, *J* = 8.78 Hz, 2 H), 8.19 (d, *J* = 7.32 Hz, 2 H), 8.80 (s, 2 H). LCMS found 363.21 [M + H]⁺.

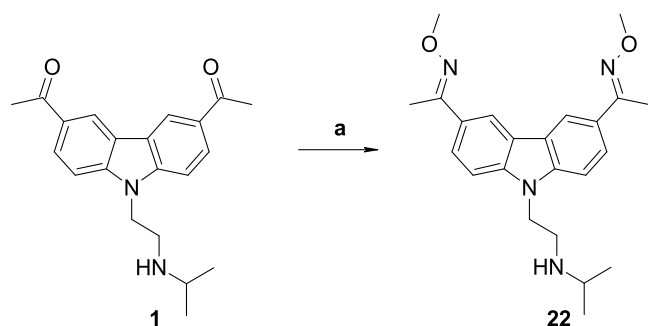
1,1'-(9-(2-(3-Fluoroazetidin-1-yl)ethyl)-9H-carbazole-3,6-diyl)bis(ethan-1-one) (**5k**). (Yield: 19%) ¹H NMR (500 MHz, CDCl₃) δ 2.75 (s, 6 H), 2.95–3.13 (m, 4 H), 3.39–3.60 (m, 2 H), 4.39 (t, *J* =

Scheme 5. Synthetic Route for Compound 15^a

^aReagents and conditions: (a) $\text{Zn}(\text{CN})_2$, Zn, $\text{Zn}(\text{OAc})_2 \cdot 2\text{H}_2\text{O}$, DMF/water (100:1), 100 °C, 20 h; (b) 2-bromoethyl 4-methylbenzenesulfonate, Cs_2CO_3 , DMF, rt, 16 h; and (c) isopropylamine, DMF, microwave 100 °C, 30 min.

Scheme 6. Synthetic Route for Compounds 21^a

^aReagents and conditions: (a) $\text{Pd}(\text{OAc})_2$, Xantphos, Cs_2CO_3 , dioxane, 100 °C, 16 h; (b) $\text{Pd}(\text{OAc})_2$, (\pm)-BINAP, Cs_2CO_3 , toluene, microwave 130 °C, 3 h; (c) $\text{Pd}(\text{OAc})_2$, Xphos, Cs_2CO_3 , toluene, 130 °C, 1 h; (d) $\text{Pd}(\text{OAc})_2$, K_2CO_3 , pivalic acid, 100 °C, air, 16 h; (e) 2-bromoethyl 4-methylbenzenesulfonate, Cs_2CO_3 , DMF, rt, 16 h; and (f) amine, DMF, microwave 100 °C, 30 min.

Scheme 7. Synthetic Route for Compound 22^a

^aReagents and conditions: (a) methoxyamine hydrochloride, ethanol, rt, 18 h.

6.34 Hz, 2 H), 4.87–5.16 (m, 1 H), 7.49 (d, $J = 8.78$ Hz, 2 H), 8.19 (dd, $J = 8.78$, 1.46 Hz, 2 H), 8.78 (d, $J = 0.98$ Hz, 2 H). LCMS found 353.24 $[\text{M} + \text{H}]^+$.

1,1'-(9-(2-(3,3-Difluoroazetidin-1-yl)ethyl)-9H-carbazole-3,6-diyl)bis(ethan-1-one) (5l). (Yield: 5.8%); ^1H NMR (500 MHz, CDCl_3) δ 2.76 (s, 6 H), 3.11 (t, $J = 5.61$ Hz, 2 H), 3.44 (t, $J = 11.96$ Hz, 4 H), 4.46 (t, $J = 6.10$ Hz, 2 H), 7.51 (d, $J = 8.30$ Hz, 2 H), 8.21 (dd, $J = 8.78$, 0.98 Hz, 2 H), 8.80 (s, 2 H). LCMS found 371.21 $[\text{M} + \text{H}]^+$.

1,1'-(9-(2-(3-Methylazetidin-1-yl)ethyl)-9H-carbazole-3,6-diyl)bis(ethan-1-one) (5m). (Yield: 22.7%); ^1H NMR (500 MHz, CDCl_3) δ 1.08 (d, $J = 6.83$ Hz, 3 H), 2.53 (d, $J = 6.83$ Hz, 1 H), 2.69 (t, $J = 6.59$ Hz, 2 H), 2.75 (s, 6 H), 2.92 (t, $J = 6.59$ Hz, 2 H), 3.41 (t, $J = 7.32$ Hz, 2 H), 4.38 (t, $J = 6.59$ Hz, 2 H), 7.52 (d, $J = 8.78$ Hz, 2 H),

8.19 (dd, $J = 8.54$, 1.22 Hz, 2 H), 8.79 (s, 2 H). LCMS found 349.17 $[\text{M} + \text{H}]^+$.

1,1'-(9-(2-Morpholinoethyl)-9H-carbazole-3,6-diyl)bis(ethan-1-one) (5n). (Yield: 14.3%); ^1H NMR (500 MHz, CDCl_3) δ 2.54 (d, $J = 4.39$ Hz, 4 H), 2.76 (s, 6 H), 2.81 (t, $J = 6.83$ Hz, 2 H), 3.67 (t, $J = 4.39$ Hz, 4 H), 4.49 (t, $J = 6.83$ Hz, 2 H), 7.49 (d, $J = 8.78$ Hz, 2 H), 8.19 (dd, $J = 8.78$, 1.46 Hz, 2 H), 8.80 (d, $J = 0.98$ Hz, 2 H). LCMS found 365.2 $[\text{M} + \text{H}]^+$.

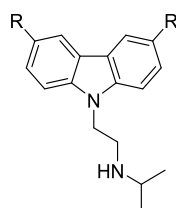
1,1'-(9-(2-(1,4-Oxazepan-4-yl)ethyl)-9H-carbazole-3,6-diyl)bis(ethan-1-one) (5o). (Yield: 22%); ^1H NMR (500 MHz, CDCl_3) δ 1.83 (br. s., 2 H), 2.73–2.82 (m, 10 H), 2.99 (br. s., 2 H), 3.64 (br. s., 2 H), 3.73 (t, $J = 6.10$ Hz, 2 H), 4.47 (br. s., 2 H), 7.49 (d, $J = 8.78$ Hz, 2 H), 8.18 (dd, $J = 8.30$, 1.46 Hz, 2 H), 8.78 (d, $J = 0.98$ Hz, 2 H). LCMS found 379.21 $[\text{M} + \text{H}]^+$.

(S)-1,1'-(9-(2-(3-Methylmorpholino)ethyl)-9H-carbazole-3,6-diyl)bis(ethan-1-one) (5p). (Yield: 28%); ^1H NMR (500 MHz, CDCl_3) δ 0.79 (br. s., 3 H), 2.44–2.57 (m, 2 H), 2.68 (br. s., 1 H), 2.76 (s, 7 H), 3.06–3.23 (m, 1 H), 3.53–3.82 (m, 3 H), 4.48 (br. s., 2 H), 7.51 (d, $J = 8.30$ Hz, 2 H), 8.19 (dd, $J = 8.78$, 1.46 Hz, 2 H), 8.79 (d, $J = 0.98$ Hz, 2 H). LCMS found 379.14 $[\text{M} + \text{H}]^+$.

(R)-1,1'-(9-(2-(3-Methylmorpholino)ethyl)-9H-carbazole-3,6-diyl)bis(ethan-1-one) (5q). (Yield: 21%); ^1H NMR (500 MHz, CDCl_3) δ 0.78 (br. s., 3 H), 2.50 (d, $J = 10.74$ Hz, 2 H), 2.61–2.70 (m, 1 H), 2.74–2.81 (m, 8 H), 3.05–3.21 (m, 2 H), 3.59 (d, $J = 11.22$ Hz, 2 H), 3.74 (br. s., 1 H), 4.45 (br. s., 2 H), 7.49 (d, $J = 8.30$ Hz, 2 H), 8.19 (dd, $J = 8.78$, 1.46 Hz, 2 H), 8.79 (d, $J = 1.46$ Hz, 2 H). LCMS found 379.14 $[\text{M} + \text{H}]^+$.

1,1'-(9-(2-Thiomorpholinoethyl)-9H-carbazole-3,6-diyl)bis(ethan-1-one) (5r). (Yield: 29%); ^1H NMR (500 MHz, CDCl_3) δ 1.26 (br. s., 4 H), 2.59 (br. s., 4 H), 2.77 (br. s., 6 H), 2.83 (d, $J = 6.34$ Hz, 2 H), 4.47 (d, $J = 6.34$ Hz, 2 H), 7.48 (d, $J = 8.30$ Hz, 2 H), 8.19

Table 5. Acetyl Replacement Analogues (Approach II): Potency, Selectivity Index, and Physicochemical and Metabolic Properties



Entry	R	<i>T. brucei</i> EC ₅₀ (μM) / (Selectivity index) ^a	<i>T. brucei</i> LLE ^b	Aq. sol. (μM)	Human Liver Microsome CL _{int} (μL/min/mg protein)	Rat hepatocyte CL _{int} (μL/min/10 ⁶ cells)
11	-Br	0.49±0.013 (10)	1.1	4	<3.0	6.1
12a		0.23±0.043 (5)	2.8	537	>300	15
12b		0.11±0.019 (28)	1.4	<5.3	<3.0	ND ^c
12c		0.057±0.013 (97)	2.1	<8.7	<3.0	15
12d		0.34±0.091 (15)	2.1	9	152	51
12e		0.11±0.013 (35)	0.38	<4.2	<3.0	6.4
12f		0.43±0.043 (11)	-1.5	<2.5	<3.0	<1
12g		>10	2.0	>1000	< 3	< 1
12h	-NHCOCH ₃	>20	--<2.5	>1000	<3.0	<1.0
12i		0.024±0.01 (138)	2.1	100	7.0	10
12j	-NH ₂	>10	2.8	482	ND ^c	ND ^c
15	-CN	0.052±0.014 (573)	3.9	21	17	7.0
21a	-COOCH ₂ C H ₃	0.030±0.009 (70)	3.1	3.0	21	>300
21b	-CF ₃	0.035±0.004 (277)	2.0	0.70	<3.0	3.4
21c	-OCF ₃	0.084±0.008 (nd)	0.49	34	<3.0	<1.0
21d		0.048±0.014 (nd)	0.71	0.2	9.6	<1.0
22		0.18±0.006(14)	3.1	60	6.0	38

^aSelectivity index = HepG2 TC₅₀/*T. brucei* EC₅₀; nd indicates not determined. ^bLipophilic ligand efficiency (LLE) = pEC₅₀ - clogP. ^cFailed to create analytical method; additional ADME data, including Log D_{7.4} and human plasma protein binding, are included in Table S1 of the Supporting Information. ND, not determined.

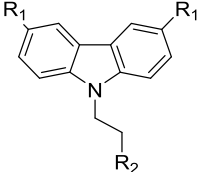
(d, *J* = 8.30 Hz, 2 H), 8.81 (br. s., 2 H). LCMS found 381.21 [M + H]⁺.

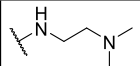
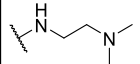
tert-Butyl 4-(2-(3,6-Diacetyl-9*H*-carbazol-9-yl)ethyl)piperazine-1-carboxylate (**5s**). (Yield: 24%): ¹H NMR (400 MHz, CD₃OD) δ 1.43 (s, 8 H), 1.47 (s, 4 H), 2.46 (br. s., 4 H), 2.74 (s, 6 H), 2.82 (t, *J* = 6.41 Hz, 2 H), 3.42 (d, *J* = 4.76 Hz, 2 H), 3.45–3.53 (m, 2 H), 4.58 (t, *J* = 6.41 Hz, 2 H), 7.67 (d, *J* = 8.79 Hz, 2 H), 8.19 (d, *J* = 8.61 Hz, 2 H), 8.91 (s, 2 H). LCMS found 464.33 [M + H]⁺.

1,1'-(9-(2-(4-Methylpiperazin-1-yl)ethyl)-9*H*-carbazole-3,6-diyl)-bis(ethan-1-one) (**5t**). (Yield: 57%): ¹H NMR (400 MHz, CD₃OD) δ 2.52 (s, 3 H), 2.57–2.82 (m, 14 H), 2.86 (t, *J* = 6.41 Hz, 2 H), 4.55 (t, *J* = 6.41 Hz, 2 H), 7.63 (d, *J* = 8.61 Hz, 2 H), 8.17 (dd, *J* = 8.61, 1.47 Hz, 2 H), 8.85 (s, 2 H). LCMS found 378.16 [M + H]⁺.

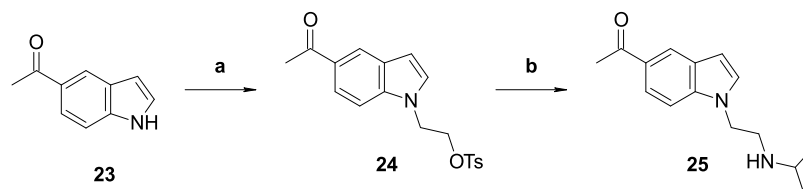
1,1'-(9-(2-(Piperazin-1-yl)ethyl)-9*H*-carbazole-3,6-diyl)bis(ethan-1-one) (**5u**). Compound **5s** was dissolved in 1 mL of dichloromethane, and 1 mL of TFA was added and stirred for 1 h. The pH

Table 6. Crossover Analogues (Approach III): Potency, Selectivity Index, and Physicochemical and Metabolic Properties



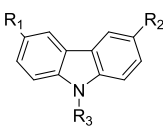
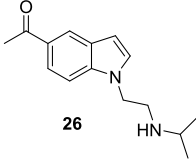
Entry	R ₁	R ₂	<i>T. brucei</i> EC ₅₀ (μM) / (Selectivity index) ^a	<i>T. brucei</i> LLE ^b	Aq. sol. (μM)	Human Liver Microsome CL _{int} (μL/min/mg protein)	Rat hepatocyte CL _{int} (μL/min/10 ⁶ cells)
21e	-CF ₃		0.049±0.009 (>10)	2.6	384	<3	3.2
21f	-OCF ₃		0.029±0.004 (ND ^b)	1.7	53	<3	<1

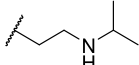
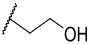
^aLipophilic ligand efficiency (LLE) = pEC₅₀ - clogP. ^bND, not determined. Additional ADME data, including Log D_{7.4} and human plasma protein binding, are included in Table S1 of the Supporting Information.

Scheme 8. Synthetic Route for Compound 26^a

^aReagents and conditions: (a) 2-bromoethyl 4-methylbenzenesulfonate, Cs₂CO₃, DMF, rt, 16 h; and (b) amine, DMF, microwave 100 °C, 30 min.

Table 7. Truncated Analogues (Approach IV): Potency, Selectivity Index, and Physicochemical and Metabolic Properties

Entry	R ₁	R ₂	R ₃	<i>T. brucei</i> EC ₅₀ (μM) / (Selectivity index) ^a	<i>T. brucei</i> LLE ^b	Aq. sol. (μM)	Human Liver Microsome CL _{int} (μL/min/mg protein)	Rat hepatocyte CL _{int} (μL/min/10 ⁶ cells)
21g	-H	-COCH ₃		0.81±0.06	2.8	>1000	22	123
6	-COCH ₃	-COCH ₃		4.8±0.58	3.6	103	118	41
3	-COCH ₃	-COCH ₃	-H	1.1±0.16	3.8	7.9	>300	41
25	-	-	-	>10	<2.4	nd	28	133

^aLipophilic ligand efficiency (LLE) = pEC₅₀ - clogP. Additional ADME data including Log D_{7.4} and human plasma protein binding are available in Table S1 of the Supporting Information.

was adjusted to neutral with 2% of NaOH solution and then extracted with dichloromethane. The organic layers were combined, dried, and washed with diethyl ether to get the product. (Yield: 61%): ¹H NMR (400 MHz, CD₃OD) 8.88 (s, 2H), 8.17–8.15 (d, J = 8 Hz, 2H), 7.66–7.63 (d, J = 12 Hz, 2H), 4.56–4.55 (m, 2H), 3.3 (m, 4H) 2.98 (m, 4H), 2.88 (m, 2H), 2.70 (s, 6H), 2.66 (m, 4H), LCMS found 364.19 [M + H]⁺.

1,1'-(9-(2-(4-Methyl-1,4-diazepan-1-yl)ethyl)-9H-carbazole-3,6-diyl)bis(ethan-1-one) (5v). (Yield: 40%): ¹H NMR (400 MHz,

CD₃OD) δ 1.72–1.79 (m, 2 H), 2.33 (s, 3 H), 2.53–2.58 (m, 2 H), 2.63–2.68 (m, 2 H), 2.71–2.81 (m, 10 H), 2.99 (t, J = 6.50 Hz, 2 H), 4.52 (t, J = 6.59 Hz, 2 H), 7.65 (d, J = 8.79 Hz, 2 H), 8.18 (dd, J = 8.61, 1.65 Hz, 2 H), 8.89 (d, J = 1.47 Hz, 2 H). LCMS found 392.32 [M + H]⁺.

1,1'-(9-(2-(2-(Dimethylamino)ethyl)amino)ethyl)-9H-carbazole-3,6-diyl)bis(ethan-1-one) (5w). (Yield: 81%): ¹H NMR (500 MHz, CDCl₃) δ 2.11 (s, 6 H), 2.30 (t, J = 6.10 Hz, 2 H), 2.64 (t, J = 5.86 Hz, 2 H), 2.68 (s, 6 H), 3.07 (t, J = 6.83 Hz, 2 H), 4.40 (t, J = 6.59

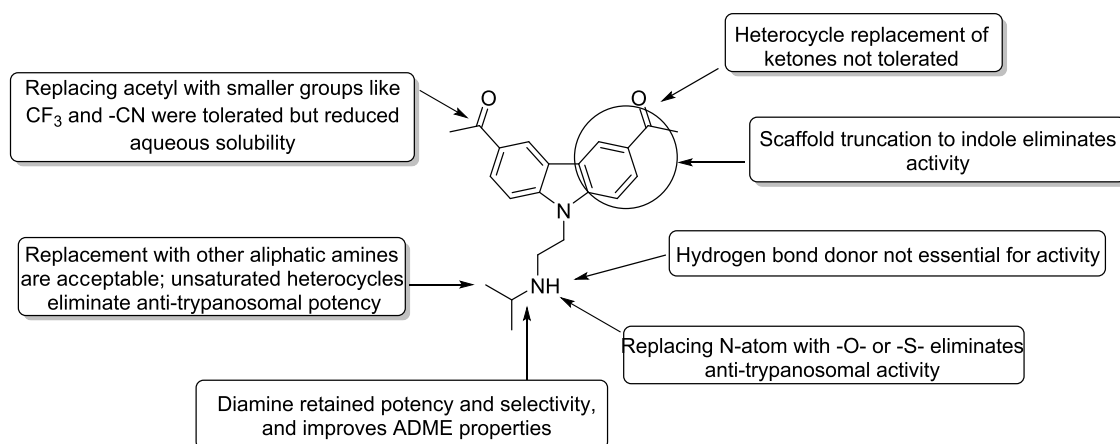


Figure 2. Key SAR and SPR points around this series for anti-*T. brucei* activity (1).

Table 8. Caco-2 Permeability, Mouse Plasma Stability, Liver Microsome Stability, and CYP450 Liability of Advanced Hits

entry	Caco-2 mean Papp A-B (10^6 cm/s)	Caco-2 mean Papp B-A (10^6 cm/s)	efflux ratio	mouse plasma stability $t_{1/2}$ (min)	mouse liver microsome (CL_{int}) (L/h/kg liver)	CYP3A4-fold induction (at $10 \mu\text{M}$)	CYP3A4% inhibition (at $10 \mu\text{M}$)
1	21	13	0.62	1200	3.1	0.17	4.6
21e	0.21	1.7	8.1	1000	0.31	0.33	21
Saf	0.63	7.4	12	680	ND	0.13	-1.2
5w	10	19	1.9	560	1.8	0.38	6.4
5h	26	25	1.0	500	4.3	0.11	4.7
5v	18	18	1.0	1200	9.2	0.17	6.3

Table 9. Candidates for Lead Discovery: Summary of New Analogs' High Selectivity Index That Meets Thresholds for Aqueous Solubility and Metabolic Stability

entry	<i>T. brucei</i> EC_{50} (μM)	selectivity index	aq. sol. (μM)	human liver microsome CL_{int} ($\mu\text{L}/\text{min}/\text{mg}$ protein)	rat hepatocyte CL_{int} ($\mu\text{L}/\text{min}/10^6$ cells)
21e	0.049 ± 0.009	224	384	<3	3.2
12i	0.024 ± 0.01	138	100	7.0	10
5v	0.10 ± 0.01	92	856	16	26
5y	0.57 ± 0.023	47	711	28	8.2
5i	0.13 ± 0.01	45	450	8.9	59
5t	0.35 ± 0.003	40	848	8.5	22
Saf	0.074 ± 0.04	36	819	<3.0	2.4
1	0.037	27	449	7.1	37

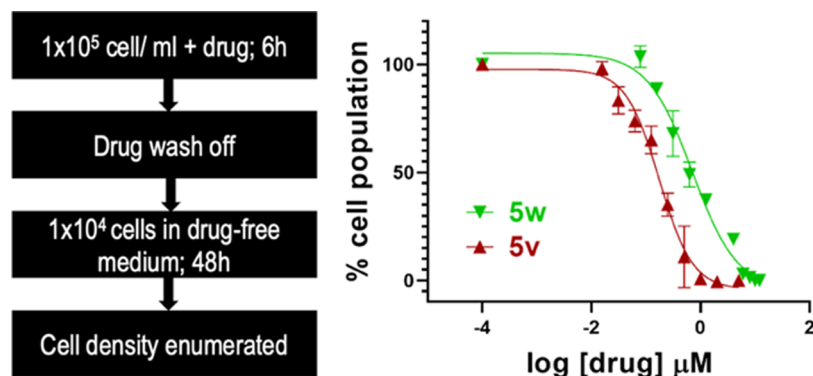


Figure 3. Delayed cytotoxic concentrations (DCCs) of 5v and 5w. *T. b. brucei* ($1 \times 10^5/\text{mL}$ HMI-9 medium) was treated with serial concentrations of 5v or 5w in 24-well plates. After 6 h, cells were washed with and transferred into a drug-free HMI-9 medium for 48 h at a starting cell density of 1×10^4 trypanosomes/mL. At the end of 48 h, trypanosomes were enumerated with a hemocytometer. Nonlinear regression graphs were constructed in GraphPad Prism to obtain DCC_{50} values.

H), 7.45 (d, $J = 8.78$ Hz, 2 H), 8.10 (dd, $J = 8.78$, 1.46 Hz, 2 H), 8.68 (s, 2 H). LCMS found 366.28 [M + H]⁺.

1,1'-(9-(2-((1-Methylpiperidin-4-yl)amino)ethyl)-9H-carbazole-3,6-diyl)bis(ethan-1-one) (5x). (Yield: 18%): ¹H NMR (500 MHz, CDCl₃) δ 1.61 (br. s., 7 H), 1.79 (d, $J = 12.69$ Hz, 2 H), 2.25 (s, 3 H),

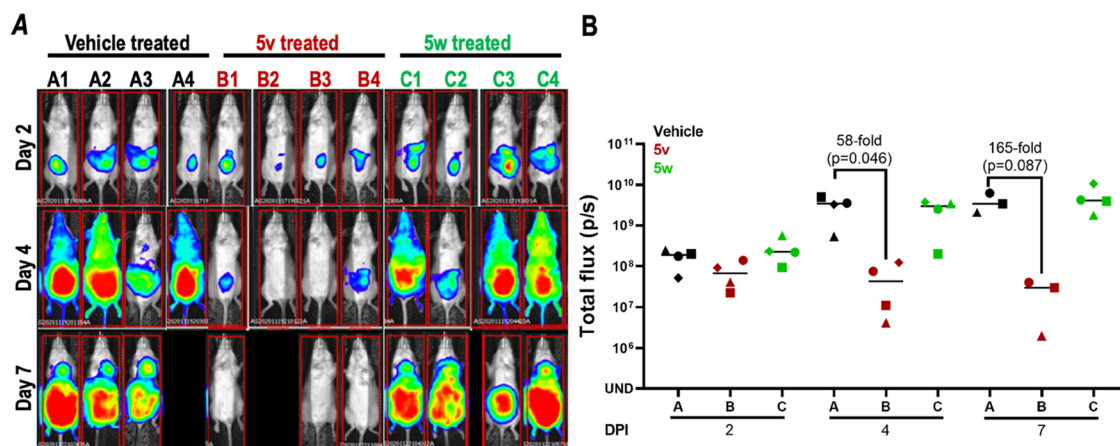


Figure 4. Efficacy of **5v** and **5w** in a mouse model of chronic HAT. Mice ($n = 4$ per group) were infected with *T. brucei* AnTat1.1 AmLuc (5×10^4). Trypanosome infection of mice was confirmed on day 0 by the detection of bioluminescence signals in all mice (data not shown). Compound **5v** was administered to mice B1–B4 (80 mg/kg on days 1, 2, 3, 4, 7, 8, 9, 10, 13, and 14 post infection). Compound **5w** was administered to mice C1–C4 (80 mg/kg on days 1, 2, 3, 4, 5, 8, 9, 10, 11, and 12 post infection). Control mice (A1–A4) received vehicle (5% NMP in 0.2% HPMC) for 10 days. For imaging, mice were injected with D-luciferin (150 mg/kg) and bioluminescence signal obtained after 12 min using an IVIS Lumina II. Images of mice were obtained at 60 s exposures. (A) Montage of infected vehicle-treated (A1–A4), infected **5v**-treated (B1–B4), and infected **5w**-treated (C1–C4) mice on different days post infection. Mice A4 and B2 died during the course of the study due to unknown causes. (B) Bioluminescence signal intensity from whole mice is presented; the bar indicates mean values. The statistical significance of differences in the total flux between untreated and drug-treated mice was analyzed with a *t*-test (Prism 5.0 software).

2.76 (s, 6 H), 3.15 (t, $J = 6.59$ Hz, 2 H), 4.49 (t, $J = 6.59$ Hz, 2 H), 7.54 (d, $J = 8.78$ Hz, 2 H), 8.19 (d, $J = 8.30$ Hz, 2 H), 8.81 (s, 2 H). LCMS found 392.32 $[M + H]^+$.

1,1'-(9-(2-(3-(Dimethylamino)azetidino)ethyl)-9H-carbazole-3,6-diyl)bis(ethan-1-one) (5y). (Yield: 17%): ^1H NMR (500 MHz, CDCl_3) δ 2.09 (s, 6 H), 2.75 (s, 6 H), 2.88 (br. s., 3 H), 2.99 (t, $J = 6.83$ Hz, 2 H), 3.35–3.50 (m, 2 H), 4.38 (t, $J = 6.59$ Hz, 2 H), 7.49 (d, $J = 8.30$ Hz, 2 H), 8.18 (dd, $J = 8.78, 1.46$ Hz, 2 H), 8.78 (d, $J = 0.98$ Hz, 2 H). LCMS found 378.16 $[M + H]^+$.

1,1'-(9-(2-(Isopropylthio)ethyl)-9H-carbazole-3,6-diyl)bis(ethan-1-one) (5z). (Yield: 12%): ^1H NMR (500 MHz, CDCl_3) δ 8.80 (br. s., 2H), 8.20 (d, $J = 8.78$ Hz, 2H), 7.51 (d, $J = 8.78$ Hz, 2H), 4.57 (t, $J = 7.32$ Hz, 2H), 2.99–3.11 (m, 2 H), 2.83–2.95 (m, 1 H), 2.76 (s, 6 H), 1.20–1.34 (m, 6 H), 1.20–1.34 (m, 6H). LCMS found 354.22 $[M + H]^+$.

1,1'-(9-(2-(1H-Imidazol-1-yl)ethyl)-9H-carbazole-3,6-diyl)bis(ethan-1-one) (5aa). (Yield: 22%): ^1H NMR (500 MHz, CDCl_3) δ 2.75 (s, 6 H), 4.47–4.52 (m, 2 H), 4.70 (d, $J = 5.49$ Hz, 2 H), 6.60 (s, 1 H), 6.92 (s, 1 H), 7.17 (d, $J = 8.23$ Hz, 2 H), 8.13 (dd, $J = 8.78, 1.65$ Hz, 2 H), 8.80 (s, 2 H). LCMS found 346.10 $[M + H]^+$.

1,1'-(9-(2-(1H-Pyrazol-1-yl)ethyl)-9H-carbazole-3,6-diyl)bis(ethan-1-one) (5ab). (Yield: 21%): ^1H NMR (500 MHz, CDCl_3) δ 2.70–2.78 (m, 6 H), 4.59 (t, $J = 5.37$ Hz, 2 H), 4.81 (t, $J = 5.37$ Hz, 2 H), 5.94 (s, 1 H), 6.69 (d, $J = 1.46$ Hz, 1 H), 7.19 (d, $J = 8.78$ Hz, 2 H), 7.56 (s, 1 H), 8.09 (dd, $J = 8.54, 1.22$ Hz, 2 H), 8.76 (s, 2 H). LCMS found 346.09 $[M + H]^+$.

Synthesis of 1,1'-(9-(2-Hydroxyethyl)-9H-carbazole-3,6-diyl)bis(ethan-1-one) (6). **1,1'-(9H-Carbazole-3,6-diyl)bis(ethan-1-one)** (compound **2**, 5.00 g, 19.9 mmol), cesium carbonate (19.5 g, 59.7 mmol), and 2-bromoethanol (3.53 mL, 49.7 mmol) were taken up in *N,N*-dimethylformamide (25 mL) and heated under stirring at 60 °C for 18 h. The reaction was diluted with water (250 mL) and extracted from ethyl acetate (3 \times 250 mL) and 5% (v/v) methanol/dichloromethane (1 \times 250 mL). The combined organic layers were dried over sodium sulfate, filtered, and evaporated to near dryness. The concentrated solution was diluted with ice-cold water (200 mL), and the yellow amorphous solid was collected by vacuum filtration to afford **1,1'-(9-(2-hydroxyethyl)-9H-carbazole-3,6-diyl)bis(ethan-1-one)** (5.24 g, 89%). ^1H NMR (500 MHz, CDCl_3) δ 8.71 (d, $J = 1.05$ Hz, 2 H), 8.13 (dd, $J = 8.64, 1.50$ Hz, 2 H), 7.53 (d, $J = 8.64$ Hz, 2 H), 4.54 (t, $J = 5.25$ Hz, 2 H), 4.14 (t, $J = 5.15$ Hz, 2 H), 2.67 (s, 6 H). LCMS: 296.1 $[M + H]^+$.

Synthesis of 2-(3,6-Diacetyl-9H-carbazol-9-yl)acetaldehyde (7). **1,1'-(9-(2-Hydroxyethyl)-9H-carbazole-3,6-diyl)bis(ethan-1-one)** (**4**, 5.27 g, 17.9 mmol) was suspended in acetonitrile (178 mL), after which Dess–Martin periodinane (8.33 g, 19.6 mmol) was added portionwise under stirring. The reaction was heated at 80 °C for 80 min in an oil bath. After removal from heat, the formed solid was removed by filtration, and the filtrate was concentrated to dryness, affording a crude light brown amorphous solid of **2-(3,6-diacetyl-9H-carbazol-9-yl)acetaldehyde** (yield 76%). ^1H NMR (500 MHz, CDCl_3) δ 9.82 (s, 1 H), 8.82 (d, $J = 1.00$ Hz, 2 H), 8.19 (dd, $J = 8.49, 1.50$ Hz, 2 H), 7.34 (d, $J = 8.49$ Hz, 2 H), 5.13 (s, 2 H), 2.75 (s, 6 H). LCMS: 312.19 $[M + \text{H}_3\text{O}]^+$.

General Method for Preparation of Compounds 5ac–al. **2-(3,6-Diacetyl-9H-carbazol-9-yl)acetaldehyde** (**7**, 0.68 mmol) was suspended in dichloroethane (7 mL) with oven-dried molecular sieves under stirring at room temperature. To this were added corresponding amine (4 equiv) and acetic acid (4 equiv). The solution was allowed to stir at room temperature for 15 min, after which sodium triacetoxyborohydride (4 equiv) was added portionwise. The reaction was allowed to stir at room temperature for another 2.5 h. After completion of the reaction monitored through the LCMS analysis, the reaction was diluted with a saturated sodium bicarbonate solution (50 mL) and extracted from 5% (v/v) methanol/dichloromethane (3 \times 50 mL). The organic layer was dried and then purified by flash chromatography using 0–50% methanol (5% ammonium hydroxide) in ethyl acetate gradient to get the desired product.

1,1'-(9-(2-(Isopropyl(methyl)amino)ethyl)-9H-carbazole-3,6-diyl)bis(ethan-1-one) (5ac). (Yield: 45%): ^1H NMR (500 MHz, CDCl_3) δ 0.86 (d, $J = 6.34$ Hz, 6 H), 2.32 (s, 3 H), 2.70 (s, 6 H), 2.73–2.79 (m, 3 H), 4.34 (t, $J = 7.08$ Hz, 2 H), 7.42 (d, $J = 8.78$ Hz, 2 H), 8.12 (d, $J = 8.78$ Hz, 2 H), 8.70 (s, 2 H). LCMS found 351.28 $[M + H]^+$.

1,1'-(9-(2-((Tetrahydro-2H-pyran-4-yl)amino)ethyl)-9H-carbazole-3,6-diyl)bis(ethan-1-one) (5ad). (Yield: 19%): ^1H NMR (500 MHz, CDCl_3) δ 1.25–1.35 (m, 2 H), 1.73 (d, $J = 12.63$ Hz, 2 H), 2.60–2.67 (m, 1 H), 2.76 (s, 6 H), 3.17 (t, $J = 6.31$ Hz, 2 H), 3.33 (td, $J = 11.53, 2.20$ Hz, 2 H), 3.79–3.98 (m, 2 H), 4.50 (t, $J = 6.31$ Hz, 2 H), 7.54 (d, $J = 8.78$ Hz, 2 H), 8.19 (dd, $J = 8.78, 1.65$ Hz, 2 H), 8.80 (d, $J = 1.10$ Hz, 2 H). LCMS found 379.17 $[M + H]^+$.

1,1'-(9-(2-((2-(Dimethylamino)ethyl)(methyl)amino)ethyl)-9H-carbazole-3,6-diyl)bis(ethan-1-one) (5ae). (Yield: 27%): ^1H NMR

(500 MHz, CDCl₃) δ 2.16 (s, 6 H), 2.26–2.31 (m, 2 H), 2.37 (s, 3 H), 2.53 (t, J = 6.83 Hz, 2 H), 2.72 (s, 6 H), 2.82 (t, J = 7.32 Hz, 2 H), 4.43 (t, J = 7.32 Hz, 2 H), 7.45 (d, J = 8.78 Hz, 2 H), 8.15 (dd, J = 8.54, 1.22 Hz, 2 H), 8.74 (d, J = 0.98 Hz, 2 H). LCMS found 380.19 [M + H]⁺.

1,1'-(9-(2-((4-(Dimethylamino)cyclohexyl)amino)ethyl)-9H-carbazole-3,6-diyl)bis(ethan-1-one) (5af). (Yield: 26%): ¹H NMR (500 MHz, DMSO-*d*₆) δ 9.04 (s, 2H), 8.11 (dd, J = 1.65, 8.78 Hz, 2H), 7.76 (d, J = 8.78 Hz, 2H), 4.49 (t, J = 6.59 Hz, 2H), 2.94 (t, J = 6.59 Hz, 2H), 2.70 (s, 6H), 2.24–2.33 (m, 1H), 2.16 (s, 6H), 2.11 (d, J = 3.29 Hz, 1H), 1.79 (d, J = 11.53 Hz, 2H), 1.71 (d, J = 12.08 Hz, 2H), 1.05–1.16 (m, J = 12.63 Hz, 2H), 0.81–0.94 (m, 2H). 1.12–.86 (m, 2H). LCMS found 420.02 [M + H]⁺.

1,1'-(9-(2-((2-(Pyrrolidin-1-yl)ethyl)amino)ethyl)-9H-carbazole-3,6-diyl)bis(ethan-1-one) (5ag). (Yield: 27%): ¹H NMR (500 MHz, CDCl₃) δ 1.72 (br. s., 4 H), 2.51 (br. s., 4 H), 2.55–2.62 (m, 2 H), 2.70–2.77 (m, 8 H), 3.10 (t, J = 6.59 Hz, 2 H), 4.45 (t, J = 6.59 Hz, 2 H), 7.50 (d, J = 8.30 Hz, 2 H), 8.14 (d, J = 8.30 Hz, 2 H), 8.75 (s, 2 H). LCMS found 392.20 [M + H]⁺.

1,1'-(9-(2-((3-(Dimethylamino)propyl)amino)ethyl)-9H-carbazole-3,6-diyl)bis(ethan-1-one) (5ah). (Yield: 15%): ¹H NMR (500 MHz, DMSO-*d*₆) δ 1.41 (s, 2 H), 1.90 (s, 3 H), 1.99 (s, 6 H), 2.12 (s, 2 H), 2.66–2.74 (m, 8 H), 2.94 (s, 2 H), 4.54 (s, 2 H), 7.78 (d, J = 8.78 Hz, 2 H), 8.11 (dd, J = 8.51, 1.37 Hz, 2 H), 9.05 (s, 2 H). LCMS found 380.26 [M + H]⁺.

1,1'-(9-(2-(4-Cyclopropylpiperazin-1-yl)ethyl)-9H-carbazole-3,6-diyl)bis(ethan-1-one) (5ai). (Yield: 17%): ¹H NMR (500 MHz, CDCl₃) δ ppm: 8.74 (s, 2H), 8.14–8.12 (d, J = 8 Hz, 2H), 7.44–7.43 (d, J = 4 Hz, 2H), 4.45–4.42 (t, J = 8 Hz, 2H), 7.759 (m, 2H), 2.70–2.52 (m, 8 Hz), 1.58–1.57 (m, 1H), 0.40 (m, 4H). LCMS found 404.21 [M + H]⁺.

1,1'-(9-(2-(4-(Oxetan-3-yl)piperazin-1-yl)ethyl)-9H-carbazole-3,6-diyl)bis(ethan-1-one) (5aj). (Yield: 10%): ¹H NMR (400 MHz, CDCl₃) δ 2.33 (br. s., 4 H), 2.60 (br. s., 4 H), 2.76 (s, 6 H), 2.83 (t, J = 7.02 Hz, 2 H), 3.48 (t, J = 6.82 Hz, 1 H), 4.49 (t, J = 7.02 Hz, 2 H), 4.56–4.62 (m, 2 H), 4.63–4.70 (m, 2 H), 7.49 (d, J = 8.58 Hz, 2 H), 8.19 (dd, J = 8.77, 1.36 Hz, 2 H), 8.80 (d, J = 0.78 Hz, 2 H). LCMS found 420.7 [M + H]⁺.

1,1'-(9-(2-(2-(Isopropylamino)ethyl)amino)ethyl)-9H-carbazole-3,6-diyl)bis(ethan-1-one) (5ak). (Yield: 12%) ¹H NMR (500 MHz, CDCl₃) δ 1.02 (s, 6H), 2.67–2.74 (m, 2H), 2.74 (s, 6H), 2.75–2.77 (m, 3H), 3.13–3.15 (m, 2H), 4.49–4.51 (m, 2H), 7.54 (d, J = 8.8 Hz, 2 H), 8.19 (d, J = 8.8, 2 H), 8.79 (s, 2 H). LCMS found 380.24 [M + H]⁺.

1,1'-(9-(2-(2-Oxa-6-azaspiro[3.3]heptan-6-yl)ethyl)-9H-carbazole-3,6-diyl)bis(ethan-1-one) (5al). (Yield: 19%). ¹H NMR (500 MHz, DMSO-*d*₆) δ 8.80 (s, 2H), 8.20–8.18 (d, J = 10 Hz, 2H), 7.49–7.47 (d, J = 10 Hz, 2H), 4.64 (s, 4H), 4.37–4.34 (t, J = 10 Hz, 2H), 3.24 (s, 4H), 2.89–2.87 (d, J = 10 Hz, 2H), 2.76 (s, 6H). LCMS found 376.5 [M + H]⁺.

Synthesis of 1,1'-(9-(2-Isopropoxyethyl)-9H-carbazole-3,6-diyl)bis(ethan-1-one) (8). 1,1'-(9H-Carbazole-3,6-diyl)bis(ethan-1-one) (2, 0.4 mmol), cesium carbonate (1.2 mmol), and 2-(2-bromoethoxy)propane (1.2 mmol) were taken up in *N,N*-dimethylformamide (1 mL) and stirred at room temperature for 16 h. The reaction was diluted with water (50 mL), and the solid was collected by vacuum filtration to afford the product (8, yield: 66%, off-white solid). ¹H NMR (500 MHz, DMSO-*d*₆) δ ppm: 0.85 (d, J = 6.04 Hz, 6 H), 2.71 (s, 6 H), 3.36–3.43 (m, 1 H), 3.76 (s, 2 H), 4.62 (s, 2 H), 7.77 (d, J = 8.78 Hz, 2 H), 8.11 (dd, J = 8.51, 1.37 Hz, 2 H), 9.05 (s, 2 H). LCMS found 338.16 [M + H]⁺.

Synthesis of 2-(3,6-Dibromo-9H-carbazol-9-yl)ethyl 4-methylbenzenesulfonate (10). A similar procedure was used as in 4b: 3,6-dibromo-9H-carbazole (2, 615 mg, 2.45 mmol), 2-bromoethyl-4-methylbenzenesulfonate (2.05 g, 7.34 mmol), and cesium carbonate (2.39 g, 7.34 mmol) were taken up in *N,N*-dimethylformamide (36 mL) under stirring at room temperature for 3 days. The reaction was diluted with water (300 mL) and extracted with ethyl acetate (5 × 100 mL). The combined organic layers were washed with a saturated brine solution. Following this, the combined organic layers were dried over sodium sulfate, filtered, and evaporated to dryness, affording a

crude yellow solid. The crude material was purified via silica gel chromatography (0–100% ethyl acetate/hexane) to afford a yellow amorphous solid of 2-(3,6-dibromo-9H-carbazol-9-yl)ethyl 4-methylbenzenesulfonate (65%). ¹H NMR (500 MHz, DMSO-*d*₆) δ 8.41 (d, J = 1.83 Hz, 2H), 7.52–7.56 (m, 2H), 7.42–7.49 (m, 2H), 6.96 (d, J = 8.24 Hz, 2H), 6.88 (d, J = 8.09 Hz, 2H), 4.64 (t, J = 4.65 Hz, 2H), 4.36 (t, J = 4.73 Hz, 2H), 2.27 (s, 3H). LCMS found 521.9 [M + H]⁺.

Synthesis of N-(2-(3,6-Dibromo-9H-carbazol-9-yl)ethyl)propan-2-amine (11). In a microwave vial were added 2-(3,6-dibromo-9H-carbazol-9-yl)ethyl 4-methylbenzenesulfonate (10, 25 mg, 70 μ mol), isopropylamine (17 mg, 140 μ mol), and anhydrous *N,N*-dimethylformamide (2 mL). The resulting reaction mixture was sealed, then evacuated, and backfilled with N₂ three times. The reaction mixture was then subjected to microwave irradiation at 100 °C for 1 h. The reaction mixture was concentrated to remove the DMF, and the crude material was purified through column chromatography using MeOH/DCM 10–90% to afford the title compound as a semi-solid, gradually turning to a brown color solid. Yield: 38%, light brown solid, ¹H NMR (500 MHz, CDCl₃) δ 8.13 (d, J = 1.7 Hz, 2H), 7.55 (dd, J = 8.7, 1.9 Hz, 2H), 7.34 (d, J = 8.7 Hz, 2H), 4.37 (t, J = 6.6 Hz, 2H), 3.04 (t, J = 6.6 Hz, 2H), 2.76 (dt, J = 12.5, 6.2 Hz, 1H), 0.99 (d, J = 6.2 Hz, 6H). LCMS found 410.95 [M + H]⁺.

General Method for Preparation of Compounds 12a–f. In a microwave vial, a mixture of intermediate *N*-(2-(3,6-dibromo-9H-carbazol-9-yl)ethyl)propan-2-amine (11, 100 mg, 0.24 mmol), corresponding boronic acid partner (3 equiv), Pd₂dba₃ (6 mol %), tricyclohexylphosphine (18 mol %), and potassium carbonate (1.22 mmol) were dissolved in DMF/water (5 mL, 3:1). The vial was sealed and subjected to microwave irradiation (130 °C, 3 h). After cooling, the mixture was diluted with EtOAc, washed with brine, dried with Na₂SO₄, and concentrated in vacuo. Purification by flash chromatography (EtOAc/hexanes gradient) affords the desired products as solid.

N-(2-(3,6-Bis(1-methyl-1H-pyrazol-4-yl)-9H-carbazol-9-yl)ethyl)propan-2-amine (12a). (Yield: 32%): ¹H NMR (500 MHz, DMSO-*d*₆) δ 8.36 (d, J = 0.9 Hz, 2H), 8.13 (s, 2H), 7.90 (s, 2H), 7.65 (dd, J = 8.5, 1.5 Hz, 2H), 7.59 (d, J = 8.5 Hz, 2H), 4.43 (t, J = 6.7 Hz, 2H), 3.89 (s, 6H), 2.94 (t, J = 6.7 Hz, 2H), 2.85–2.75 (m, 1H), 0.96 (d, J = 6.2 Hz, 6H). LCMS found 413.17 [M + H]⁺.

N-(2-(3,6-Bis(5-methylfuran-2-yl)-9H-carbazol-9-yl)ethyl)propan-2-amine (12b). (Yield: 28%): ¹H NMR (500 MHz, CDCl₃) δ 8.40 (d, J = 1.0 Hz, 2H), 7.75 (dd, J = 8.5, 1.4 Hz, 2H), 7.43 (d, J = 8.6 Hz, 2H), 6.55 (d, J = 3.0 Hz, 2H), 6.09 (d, J = 2.1 Hz, 2H), 4.43 (t, J = 6.6 Hz, 2H), 3.10 (t, J = 6.6 Hz, 2H), 2.83–2.74 (m, 1H), 2.43 (s, 6H), 1.01 (d, J = 6.2 Hz, 7H). LCMS found 413.15 [M + H]⁺.

N-(2-(3,6-Di(furan-2-yl)-9H-carbazol-9-yl)ethyl)propan-2-amine (12c). (Yield: 22%): ¹H NMR (500 MHz, CDCl₃) δ 8.44 (d, J = 1.0 Hz, 2H), 7.80 (dd, J = 8.5, 1.5 Hz, 2H), 7.51 (d, J = 0.9 Hz, 2H), 7.47 (d, J = 8.6 Hz, 2H), 6.67 (d, J = 3.0 Hz, 2H), 6.52 (dd, J = 3.2, 1.8 Hz, 2H), 4.46 (t, J = 6.6 Hz, 2H), 3.11 (t, J = 6.6 Hz, 2H), 2.81 (dt, J = 12.4, 6.2 Hz, 1H), 1.03 (d, J = 6.2 Hz, 6H). LCMS found 365.11 [M + H]⁺.

N-(2-(3,6-Bis(3,5-dimethylisoxazol-4-yl)-9H-carbazol-9-yl)ethyl)propan-2-amine (12d). (Yield: 15%): ¹H NMR (500 MHz, CDCl₃) δ 7.95 (d, J = 0.9 Hz, 2H), 7.56 (d, J = 8.4 Hz, 2H), 7.36 (dd, J = 8.4, 1.5 Hz, 2H), 4.50 (t, J = 6.7 Hz, 2H), 3.15 (t, J = 6.7 Hz, 2H), 2.89–2.81 (m, 1H), 2.45 (s, 6H), 2.31 (s, 6H), 1.06 (d, J = 6.2 Hz, 6H). LCMS found 445.11 [M + H]⁺.

N-(2-(3,6-Di(Thiophen-2-yl)-9H-carbazol-9-yl)ethyl)propan-2-amine (12e). (Yield: 32%): ¹H NMR (500 MHz, CDCl₃) δ 8.35 (d, J = 1.2 Hz, 2H), 7.75 (dd, J = 8.5, 1.6 Hz, 2H), 7.47 (d, J = 8.5 Hz, 2H), 7.39–7.35 (m, 2H), 7.28 (d, J = 5.1 Hz, 2H), 7.12 (dd, J = 5.0, 3.6 Hz, 2H), 4.45 (t, J = 6.6 Hz, 2H), 3.11 (t, J = 6.6 Hz, 2H), 2.81 (dt, J = 12.5, 6.2 Hz, 1H), 1.03 (d, J = 6.2 Hz, 6H). LCMS found 447.22 [M + H]⁺.

N-(2-(3,6-Bis(5-methylthiophen-2-yl)-9H-carbazol-9-yl)ethyl)propan-2-amine (12f). (Yield: 34%): ¹H NMR (500 MHz, CDCl₃) δ 8.26 (d, J = 1.2 Hz, 2H), 7.68 (dd, J = 8.5, 1.6 Hz, 2H), 7.42 (d, J = 8.5 Hz, 2H), 7.15 (d, J = 3.4 Hz, 2H), 6.76 (dd, J = 3.2, 0.8 Hz, 2H), 4.42 (t, J = 6.6 Hz, 2H), 3.09 (t, J = 6.6 Hz, 2H), 2.80 (dt, J = 12.4,

6.2 Hz, 1H), 2.55 (s, 6H), 1.02 (d, $J = 6.2$ Hz, 6H). LCMS found 367.15 $[M + H]^+$.

General Method for Preparation of Compounds 12g–i. In a microwave vial, a mixture of intermediate *N*-(2-(3,6-dibromo-9*H*-carbazol-9-yl)ethyl)propan-2-amine (**11**, 50 mg, 121.91 mmol), corresponding amine partner (4 equiv), Pd₂dba₃ (20 mol %), *t*-BuXPhos (20 mol %), and potassium 2-methylpropan-2-olate (1.22 mmol) were dissolved in 10 mL of dioxane and purged with nitrogen gas for 5 min. The vial was sealed and subjected to microwave irradiation (110 °C, 35 min). After the completion of the reaction, the reaction mass was filtered through celite. The mixture was diluted with EtOAc, washed with brine, dried with Na₂SO₄, and concentrated in vacuo. Purification by flash chromatography (5% NH₄OH) and DCM gradient affords the desired products as solid.

N-(2-(3,6-Di(2-oxa-6-azaspiro[3.3]heptan-6-yl)-9*H*-carbazol-9-yl)ethyl)propan-2-amine (**12g**). (Yellow solid, 47% yield), ¹H NMR (500 MHz, DMSO-*d*₆) δ ppm: 7.37–7.34 (d, $J = 15$ Hz, 2H), 7.10 (s, 2H), 6.63–6.61 (d, $J = 10$ Hz, 2H), 4.75 (s, 8H), 3.98 (s, 8H), 4.27–4.24 (t, $J = 10$ Hz, 2H), 2.81–2.78 (t, $J = 15$ Hz, 2H), 2.78 (m, 1H), 0.92–0.90 (d, $J = 10$ Hz, 6H). LCMS found 446.6 $[M + H]^+$.

N,N'-(9-(2-(isopropylamino)ethyl)-9*H*-carbazole-3,6-diyl)-diacetamide (**12h**). (Green solid 22%), ¹H NMR (500 MHz, DMSO-*d*₆) δ ppm: 9.93 (s, 2H), 8.35 (s, 2H), 7.50 (s, 4H), 4.36–4.33 (t, $J = 5$ Hz, 2H), 2.88–2.85 (t, $J = 10$ Hz, 2H), 2.80 (s, 1H), 2.07 (s, 6H), 0.91–0.90 (d, $J = 5$ Hz, 6H). LCMS: m/z calcd 366.47 $[M + H]^+$ for C₂₁H₂₆N₄O₂ + H⁺ (367.15).

Di-tert-butyl-(9-(2-(isopropylamino)ethyl)-9*H*-carbazole-3,6-diyl)dicarbamate (**12i**). (Off-white solid, 54%), ¹H NMR (500 MHz, DMSO-*d*₆) δ ppm: 8.09 (s, 2H), 7.37 (s, 4H), 6.54 (s, 2H), 4.44 (s, 2H), 3.06 (s, 2H), 2.82 (m, 1H), 1.56 (s, 18H), 1.04 (s, 6H). LCMS: m/z calcd 282.63 $[M + H]^+$ for C₂₇H₃₈N₄O₄ + H⁺ (483.21).

Synthesis of 9-(2-(isopropylamino)ethyl)-9*H*-carbazole-3,6-diamine (12j**).** To a solution of di-tert-butyl (9-(2-(isopropylamino)ethyl)-9*H*-carbazole-3,6-diyl)dicarbamate (50 mg, 103.60 μ mol) in 5 mL of dioxane, HCl in dioxane was added at RT and the reaction mass was stirred overnight. LCMS shows the complete conversion. The reaction mass was neutralized with saturated sodium bicarbonate. The product was extracted with DCM and purified with flash chromatography in 5% ammonia in methanol and dichloromethane. Yield: 21 mg (brown solid, 72%), ¹H NMR (500 MHz, DMSO-*d*₆) δ ppm: 7.17–7.16 (d, $J = 5$ Hz, 2H), 7.016 (s, 2H), 6.73–6.71 (d, $J = 10$ Hz, 2H), 4.60 (s, 4H), 4.18–4.16 (t, $J = 5$ Hz, 2H), 2.79–2.78 (t, $J = 5$ Hz, 2H), 2.77 (m, 1H), 0.92–0.90 (d, $J = 10$ Hz, 6H). LCMS: m/z calcd 282.39 $[M + H]^+$ for C₁₇H₂₂N₄ + H⁺ (283.20).

Synthesis of 9*H*-Carbazole-3,6-dicarbonitrile (13**).**¹² To a mixture of DMF (30 mL) and water (0.3 mL) in a 150 mL round-bottom flask, 3,6-dibromo-9*H*-carbazole (5 g) and dppf (40 mg, 0.48 mol %) were added. The resulting reaction mixture was bubbled with argon for 45 min. Subsequently, Zn(CN)₂ (2.1 g, 1.2 equiv), Zn (39 mg, 4 mol %), Zn(OAc)₂ (110 mg, 4 mol %), and Pd₂(dba)₃ (27.5 mg, 0.2 mol %) were added in one portion in the presence of argon. The flask was placed in a preheated oil bath (100 °C), and the mixture was vigorously stirred for 20 h. The mixture was cooled, poured into aq NH₄Cl (4:1:5, 100 mL), and filtered. The filter cake was washed again with the same volume of the above mixture and then thoroughly with DI water, followed by toluene (3 \times 30 mL) and MeOH (3 \times 30 mL), and then dried under air with suction. A pale-yellow solid was obtained; yield: 3.1 g (96%). LCMS found 218.1 $[M + H]^+$.

Synthesis of 9-(2-(isopropylamino)ethyl)-9*H*-carbazole-3,6-dicarbonitrile (15**).** Compound **15** was synthesized from intermediate **14**, which was synthesized with the procedure as reported above for **4b** and used as such without any purification for the next step. In a microwave vial, compound **15** (25 mg, 70 μ mol), isopropylamine (17 mg, 140 μ mol), and anhydrous *N,N*-dimethylformamide (2 mL) were added. The resulting reaction mixture was sealed, then evacuated, and backfilled with N₂ three times. The reaction mixture was then subjected to microwave irradiation at 100 °C for 1 h. The reaction mixture was concentrated to remove the DMF, and the crude material was purified through column chromatography using MeOH/DCM 10–90% to afford the title compound as a semi-solid, which gradually

turned to a brown color solid (21.5 mg, 70%). ¹H NMR (500 MHz, CDCl₃) δ 1.00 (d, $J = 6.34$ Hz, 6 H), 2.77 (dt, $J = 12.32, 6.28$ Hz, 1 H), 3.10 (t, $J = 6.59$ Hz, 2 H), 4.48 (t, $J = 6.59$ Hz, 2 H), 7.61 (d, $J = 8.78$ Hz, 2 H), 7.80 (d, $J = 8.30$ Hz, 2 H), 8.42 (s, 2 H). LCMS found 303.14 $[M + H]^+$.

General Procedure for the Synthesis of Biaryl Compounds (18). In a reaction vial, 4-iodo-substituted benzene derivatives (0.38 g, 2.03 mmol), substituted anilines (0.391 g, 2.41 mmol), and Cs₂CO₃ (0.913 g, 2.80 mmol) were added sequentially to anhydrous toluene (6 mL) and the reaction mixture was degassed with nitrogen three times. Then, the ligand (0.017 mmol) and Pd(OAc)₂ (0.0133 g, 0.059 mmol) were added. The resulting reaction mixture was stirred at 100 °C (external) under N₂ for 20 h, filtered using celite, and diluted with ethyl acetate (100 mL). The brown reaction mixture was washed with water followed by brine. The resulting mixture was dried over Na₂SO₄ and evaporated to give a dark green oil, and the crude was purified using chromatography, eluting with 5% EtOAc–hexane, affording the biaryl compounds as a pale-yellow oil.

Diethyl-4,4'-azanediyldibenzoate (18a). (Yield: 38%); ¹H NMR (500 MHz, DMSO-*d*₆) δ ppm: 9.15 (s, 1H), 7.60–7.58 (d, $J = 10$ Hz, 2H), 7.28–7.26 (d, $J = 10$ Hz, 2H). LCMS found 314.35 $[M + H]^+$.

Bis(4-(trifluoromethyl)phenyl)amine (18b).¹³ Off-white solid (yield: 45%); ¹H NMR (500 MHz, DMSO-*d*₆) δ ppm: 9.15 (s, 1H), 7.60–7.58 (d, $J = 10$ Hz, 2H), 7.28–7.26 (d, $J = 10$ Hz, 2H). LCMS: found 306.97 $[M + H]^+$.

Bis(4-(trifluoromethoxy)phenyl)amine (18c).¹⁴ Off-white solid (yield: 41%); ¹H NMR (500 MHz, DMSO-*d*₆) δ ppm: (8.54, s, 1H), 7.60–7.58 (d, $J = 10$ Hz, 2H), 7.28–7.26 (d, $J = 10$ Hz, 2H); LCMS found 336.01 $[M - H]^-$.

Bis(4-(1-(trifluoromethyl)cyclopropyl)phenyl)amine (18d). Off-white solid (yield: 36%); (yield: 46%); ¹H NMR (500 MHz, DMSO-*d*₆) δ ppm: 8.40 (s, 1H), 7.31–7.29 (d, $J = 10$ Hz, 4H), 7.07–7.05 (d, $J = 10$ Hz, 4H), 1.28–1.27 (m, 4H), 1.04 (s, 4H). LCMS found 386.18 $[M + H]^+$.

General Procedure for Intramolecular Cyclization (19). Biaryl compound (**19**, 0.5 mmol), Pd(OAc)₂ (2–10 mol %), K₂CO₃ (10 mol %), and pivalic acid (30 equiv) were weighed in air and transferred into a 20 mL reaction vial. The uncapped reaction vial was placed in an oil bath, and the mixture was stirred under air at the indicated temperature and time. The solution was then cooled to rt, diluted with CH₂Cl₂, washed with a saturated aqueous solution of Na₂CO₃, dried over MgSO₄, filtered, and evaporated under reduced pressure. The crude product was purified by silica gel column chromatography to afford the corresponding coupling product.

*Diethyl-9*H*-carbazole-3,6-dicarboxylate (19a)*.¹⁵ (Yield: 73%); ¹H NMR (500 MHz, DMSO-*d*₆) δ ppm: 12.10 (s, 1H), 8.91 (s, 2H), 8.08–8.06 (d, $J = 10$ Hz, 2H), 7.63–7.61 (d, $J = 10$ Hz, 2H), 4.38 (q, $J = 12$ Hz, 4H), 1.40–1.37 (t, $J = 10$ Hz, 6H); LCMS found 310.07 $[M - H]^-$.

*3,6-Bis(trifluoromethyl)-9*H*-carbazole (19b)*. Off-white solid, ¹H NMR (500 MHz, DMSO-*d*₆) δ ppm: 12.14 (s, 1H), 8.81 (br s, 2H), 7.75–7.71 (m, 4H). LCMS found 303.21 $[M + H]^+$.

*3,6-Bis(trifluoromethoxy)-9*H*-carbazole (19c)*.¹⁶ LCMS found 336.1 $[M + H]^+$.

*3,6-Bis(1-(trifluoromethyl)cyclopropyl)-9*H*-carbazole (19d)*. ¹H NMR (500 MHz, DMSO-*d*₆) δ ppm: 11.43 (s, 1H), 8.28 (s, 2H), 7.48 (s, 4H), 1.39–1.37 (t, $J = 5$ Hz, 4H), 1.21 (m, 4H); LCMS found 382.17 $[M - H]^-$.

General Procedure for the Synthesis of Compounds 21. Compounds **21** were synthesized from intermediate **20**, which was synthesized with the procedure as reported above for **4b** and used as such without any purification for the next step. In a microwave vial, 3,6-di-substituted carbazole-ethyl 4-methylbenzenesulfonate (25 mg, 70 μ mol), isopropylamine (17 mg, 140 μ mol), and anhydrous *N,N*-dimethylformamide (2 mL) were added. The resulting reaction mixture was sealed, then evacuated, and backfilled with N₂ three times. The reaction mixture was then subjected to microwave irradiation at 100 °C for 1 h. The reaction mixture was concentrated to remove the DMF, and the crude material was purified through

column chromatography using MeOH/DCM 10–90% to afford the title compound as solids.

Diethyl-9-(2-(isopropylamino)ethyl)-9H-carbazole-3,6-dicarboxylate (21a). (Yield: 47%): $^1\text{H NMR}$ (500 MHz, CDCl_3) δ 8.86 (d, J = 1.1 Hz, 2H), 8.21 (dd, J = 8.6, 1.6 Hz, 2H), 7.50 (d, J = 8.7 Hz, 2H), 4.51–4.40 (m, 7H), 3.10 (t, J = 6.6 Hz, 2H), 2.78 (dt, J = 12.4, 6.2 Hz, 1H), 1.46 (t, J = 7.1 Hz, 7H), 1.00 (d, J = 6.2 Hz, 6H). LCMS found 397.25 $[\text{M} + \text{H}]^+$.

***N*-(2-(3,6-Bis(trifluoromethyl)-9H-carbazol-9-yl)ethyl)propan-2-amine (21b).** (Yield: 36%): $^1\text{H NMR}$ (500 MHz, CDCl_3) δ 1.04 (d, J = 6.34 Hz, 6 H), 2.82 (dt, J = 12.57, 6.16 Hz, 1 H), 3.12 (t, J = 6.59 Hz, 2 H), 4.53 (t, J = 6.59 Hz, 2 H), 7.61 (d, J = 8.30 Hz, 2 H), 7.77 (d, J = 8.30 Hz, 2 H), 8.41 (s, 2 H). LCMS found 389.13 $[\text{M} + \text{H}]^+$.

***N*-(2-(3,6-Bis(trifluoromethoxy)-9H-carbazol-9-yl)ethyl)propan-2-amine (21c).** (Yield: 25%): $^1\text{H NMR}$ (500 MHz, CDCl_3) δ 7.93 (s, 2H), 7.49 (d, J = 8.9 Hz, 2H), 7.39 (d, J = 8.8 Hz, 2H), 4.48 (t, J = 6.6 Hz, 2H), 3.11 (t, J = 6.7 Hz, 2H), 2.83 (dt, J = 12.4, 6.2 Hz, 1H), 1.06 (d, J = 6.2 Hz, 6H). LCMS found 421.11 $[\text{M} + \text{H}]^+$.

***N*-(2-(3,6-Bis(1-(trifluoromethyl)cyclopropyl)-9H-carbazol-9-yl)ethyl)propan-2-amine (21d).** (Yield: 22%): $^1\text{H NMR}$ (400 MHz, $\text{DMSO}-d_6$) δ ppm: 8.32 (br s, 2H), 7.63–7.53 (m, 4H), 4.42–4.40 (br, s, 2H), 2.88–2.86 (br, s, 2H), 2.73 (m, 1H), 1.38 (br, s, 4H), 1.21 (br, s, 4H), 0.93–0.92 (s, 6H); LCMS found 469.13 $[\text{M} + \text{H}]^+$.

***N*1-(2-(3,6-Bis(trifluoromethyl)-9H-carbazol-9-yl)ethyl)-*N*2,*N*2-dimethylethane-1,2-diamine (21e).** (Yield: 72%): $^1\text{H NMR}$ (500 MHz, CDCl_3) δ 8.42 (s, 2H), 7.78 (d, J = 8.5 Hz, 2H), 7.61 (d, J = 8.6 Hz, 2H), 4.53 (t, J = 6.7 Hz, 2H), 3.13 (t, J = 6.7 Hz, 2H), 2.70 (t, J = 6.0 Hz, 2H), 2.39 (t, J = 5.9 Hz, 2H), 2.19 (s, 6H). LCMS found 418.22 $[\text{M} + \text{H}]^+$.

***N*1-(2-(3,6-Bis(trifluoromethoxy)-9H-carbazol-9-yl)ethyl)-*N*2,*N*2-dimethylethane-1,2-diamine (21f).** (Yield: 35%): $^1\text{H NMR}$ (500 MHz, CDCl_3) δ 7.93 (s, 2H), 7.49 (d, J = 8.9 Hz, 2H), 7.39 (d, J = 8.8 Hz, 2H), 4.47 (t, J = 6.7 Hz, 2H), 3.11 (t, J = 6.7 Hz, 2H), 2.71 (t, J = 6.0 Hz, 2H), 2.41 (t, J = 6.0 Hz, 2H), 2.20 (s, 6H). LCMS found 450.16 $[\text{M} + \text{H}]^+$.

1-(9-(2-(isopropylamino)ethyl)-9H-carbazol-3-yl)ethan-1-one (21g). (Yield: 60%): $^1\text{H NMR}$ (500 MHz, CDCl_3) δ 8.76 (s, 1H), 8.20–8.11 (m, 2H), 7.52 (dd, J = 13.4, 6.9 Hz, 3H), 7.36–7.30 (m, 1H), 4.49 (t, J = 6.7 Hz, 2H), 3.12 (t, J = 6.7 Hz, 2H), 2.82 (dt, J = 12.5, 6.2 Hz, 1H), 2.74 (s, 3H), 1.04 (d, J = 6.2 Hz, 6H). LCMS found 295.25 $[\text{M} + \text{H}]^+$.

Synthesis of (1*E*,1'*E*)-1,1'-(9-(2-(isopropylamino)ethyl)-9H-carbazole-3,6-diyl)bis(ethan-1-one)-*O*,*O*-dimethyl-dioxime (22). Compound **1** (50.0 mg, 149 μmol) and methoxyamine hydrochloride (99.3 mg, 1.19 mmol) were taken up in ethanol (4 mL) and water (0.6 mL) and allowed to stir at room temperature for 24 h. The reaction was evaporated to dryness under reduced pressure and then taken up in a biphasic system of 5% methanol/dichloromethane (100 mL) and water (100 mL). The phases were separated, after which the aqueous layer was extracted with 5% methanol/dichloromethane (1 \times 100 mL). The combined organic layers were dried over magnesium sulfate, filtered, and then evaporated to dryness. The crude material was purified via silica gel chromatography (0–10% methanol/dichloromethane) to afford the desired product **22** (yield: 17%). $^1\text{H NMR}$ (500 MHz, CDCl_3) ppm, 1.01 (d, J = 6.34 Hz, 6 H), 2.38 (s, 6 H), 2.78 (dq, J = 12.50, 5.92 Hz, 1 H), 3.09 (t, J = 6.59 Hz, 2 H), 4.06 (s, 6 H), 4.46 (t, J = 6.59 Hz, 2 H), 7.46 (d, J = 8.30 Hz, 2 H), 7.85 (dd, J = 8.54, 1.71 Hz, 2 H), 8.38 (d, J = 1.46 Hz, 2 H). LCMS found 395.34 $[\text{M} + \text{H}]^+$.

Synthesis of 2-(5-Acetyl-1*H*-indol-1-yl)ethyl 4-Methylbenzenesulfonate (24). 1,1'-(9H-Carbazole-3,6-diyl)bis(ethan-1-one) 5-acetylindole (**23**, 100 mg, 0.628 mmol), 2-bromoethyl-4-methylbenzenesulfonate (701 mg, 2.51 mmol), and Cs_2CO_3 (614 mg, 1.88 mmol) were added to a vial. To this, *N,N*-dimethylformamide (5 mL) was added and stirred at room temperature for 16 h. On completion, the reaction was then diluted with water (50 mL) and extracted with EtOAc (3 \times 50 mL). The organic layers were combined, dried over Na_2SO_4 , and purified by using normal phase with ethyl acetate in hexane gradient to yield the product as an off-white solid (108 mg, 48% yield). $^1\text{H NMR}$ (500 MHz, CDCl_3) δ 8.34 (s, 1H), 7.82 (dd, J = 10, 5.0 Hz, 1H), 7.63 (d, J = 10 Hz, 1H), 7.51 (d, J = 5.0 Hz, 1H),

7.38 (d, J = 8.3 Hz, 2H), 7.22 (d, J = 8.3 Hz, 2H), 6.64 (d, J = 5.0 Hz, 1H), 4.41 (t, J = 5.0 Hz, 2H), 3.91 (t, J = 5.0 Hz, 2H), 2.51 (s, 3H), 2.36 (s, 3H). LCMS: 358.3 $[\text{M} + \text{H}]^+$.

Synthesis of 1-(1-(2-(isopropylamino)ethyl)-1*H*-indol-5-yl)ethan-1-one (25). 2-(5-Acetyl-1*H*-indol-1-yl)ethyl 4-methylbenzenesulfonate (**24**, 100 mg, 0.28 mmol) was dissolved in *N,N*-dimethylformamide (1 mL) and isopropylamine (165.4 mg, 2.8 mmol) was added to it. The reaction was then heated in a microwave at 100 $^\circ\text{C}$ for 30 min. The reaction was then diluted with water (50 mL) and extracted with EtOAc (3 \times 50 mL). The organic layers were combined, dried over Na_2SO_4 , and purified by using normal phase with methanol in dichloromethane gradient to yield the product as a white solid (28 mg, 41% yield). $^1\text{H NMR}$ (500 MHz, $\text{DMSO}-d_6$) δ 8.22 (s, 1H) 7.71 (dd, J = 10, 5.0 Hz, 1H), 7.53 (d, J = 10 Hz, 1H), 7.47 (d, J = 5.0 Hz, 1H), 6.56 (d, J = 5.0 Hz, 1H), 4.20 (t, J = 5.0 Hz, 2H), 2.83 (t, J = 5.0 Hz, 2H), 2.64–2.59 (m, 1H), 2.45 (s, 3H), 0.87 (d, J = 10 Hz, 6H). LCMS: 245.1 $[\text{M} + \text{H}]^+$.

Proliferation Inhibition Assay for *T. b. brucei*. *T. b. brucei* Lister 427 was inoculated at 4×10^3 cells/mL or 2×10^3 cells/mL (in 50 μL HMI-9 medium), respectively, into a 384-well black plate (Greiner; Frickenhausen, Germany). Each compound was serially diluted in duplicate wells. Plates were incubated for 48 h at 37 $^\circ\text{C}$ and 5% CO_2 . Cells were lysed by adding 15 μL of 1 \times SYBR Green I (Invitrogen; Carlsbad, CA) in lysis solution (30 mM tris pH 7.5, 7.5 mM EDTA, 0.012% saponin, and 0.12% Triton X-100) to each well followed by incubation in the dark for 1 h at room temperature.¹⁰ Fluorescence in lysates was quantitated (100 ms; λ_{ex} : 485 nm, λ_{em} : 538 nm) with a Fluoroskan Ascent microplate fluorometer (Thermo Scientific). Each experiment was performed thrice. Nonlinear regression graphs of data were plotted with GraphPad Prism (GraphPad Software; La Jolla, CA) to determine GI_{50} (drug concentration that inhibits trypanosome proliferation by 50%).

Delayed Cytocidal Assay for *T. b. brucei*. Mid-logarithmic growth-phase *T. brucei* Lister 427 was inoculated into HMI-9 medium (1×10^5 cell/mL). Cells were incubated with either 0.1% dimethyl sulfoxide (DMSO) (vehicle) or serial dilutions of compounds in 24-well plates for 6 h at 37 $^\circ\text{C}$ /5% CO_2 , following which HMI-9 medium was removed by pelleting trypanosomes (3000g, 5 min) and rinsing with drug-free HMI-9 medium. Trypanosomes were then inoculated at 1×10^4 cells/mL in 24-well plates and cultured for 48 h at 37 $^\circ\text{C}$ /5% CO_2 . At the end of 48 h, trypanosomes were enumerated with a hemocytometer. Nonlinear regression graphs were analyzed with GraphPad Prism to obtain DCC_{50} and DCC_{90} values.

Repetitive Maximum Tolerated Dose (rMTD) of Hits. Repetitive maximum tolerated dose studies of **5v** were performed by Buffalo Biolabs, a contract research organization. Swiss-Webster mice (male and female; 8–9 weeks old) were administered **5v** or **5w** (formulated in 0.2% hydroxypropyl methylcellulose) at 30, 60, and 120 mg/kg orally each day for a total of 10 doses. Control mice received vehicle alone. Mice were monitored daily for the overall condition (base parameters presented in Table S2) and body weight changes for up to 7 days post administration of the drug. After the study, mice were euthanized by CO_2 asphyxiation followed by cervical dislocation.

Efficacy of **5v in a Mouse Model of Chronic HAT.** Mid-logarithmic (below $5 \times 10^5/\text{mL}$) *T. brucei* AnTat1.1 AmLuc line expressing firefly luciferase¹⁷ was maintained in HMI-9. For infection (day 0), female Swiss-Webster mice (8–10 weeks old, 20–25 g, $n = 4$ per group, two groups) received 5×10^4 trypanosomes intraperitoneally (i.p.) in 100 μL of HMI-9 medium using 26G needles. Starting on day 1 post infection, group A was given 10 mL/kg of vehicle alone (5% NMP in 0.2% HPMC) for 10 days. Group B was given **5v** (80 mg/kg in vehicle) on days 1, 2, 3, 4, 7, 8, 9, 10, 13, and 14. To determine the tissue load of trypanosomes, mice received intraperitoneal injection of D-luciferin (150 mg/kg)¹⁷ and were anesthetized under 2.5% isoflurane mixed with medical grade oxygen. After 12 min, images of mice were obtained using an IVIS Lumina II system. A hit producing >100-fold reduction in trypanosome bioluminescence in mice was considered a lead for drug development. All experiments with mice were conducted with the approval of the

Institutional Animal Care and Use Committee (IACUC) at the University of Georgia. During the study, mice with signs of illness or relapsing parasite load were euthanized by CO₂ overdose followed by an incision to form a bilateral pneumothorax.

Compound **5w** was administered to mice group C (80 mg/kg in vehicle) on days 1, 2, 3, 4, 5, 8, 9, 10, 11, and 12 post infection. Control mice (A1–A4) received vehicle (5% NMP in 0.2% HPMC) for 10 days.

For imaging, mice were injected with D-luciferin (150 mg/kg) and a bioluminescence signal was obtained after 12 min using an IVIS Lumina II. Images of mice were obtained at 60 s of exposure.

■ ASSOCIATED CONTENT

SI Supporting Information

The Supporting Information is available free of charge at <https://pubs.acs.org/doi/10.1021/acs.jmedchem.2c01767>.

Supplemental biological and ADME data (annotated with NEU registry numbers), experiment protocols, and HPLC trace of the compounds tested *in vivo* (**5v**, **5w**) (PDF)

Molecular strings (CSV)

■ AUTHOR INFORMATION

Corresponding Authors

Kojo Mensa-Wilmot – Department of Molecular and Cellular Biology, Kennesaw State University, Kennesaw, Georgia 30144, United States; Center for Tropical and Emerging Global Diseases, University of Georgia, Athens, Georgia 30602, United States; Email: kmensawi@kennesaw.edu

Michael P. Pollastri – Department of Chemistry and Chemical Biology, Northeastern University, Boston, Massachusetts 02115, United States; orcid.org/0000-0001-9943-7197; Email: m.pollastri@northeastern.edu

Authors

Baljinder Singh – Department of Chemistry and Chemical Biology, Northeastern University, Boston, Massachusetts 02115, United States; orcid.org/0000-0003-2828-5768

Amrita Sharma – Department of Molecular and Cellular Biology, Kennesaw State University, Kennesaw, Georgia 30144, United States

Naresh Gunaganti – Department of Chemistry and Chemical Biology, Northeastern University, Boston, Massachusetts 02115, United States

Mitch Rivers – Department of Chemistry and Chemical Biology, Northeastern University, Boston, Massachusetts 02115, United States

Pradip K. Gadekar – Department of Chemistry and Chemical Biology, Northeastern University, Boston, Massachusetts 02115, United States; orcid.org/0000-0002-9129-8812

Brady Greene – Department of Chemistry and Chemical Biology, Northeastern University, Boston, Massachusetts 02115, United States

Michael Chichioco – Department of Chemistry and Chemical Biology, Northeastern University, Boston, Massachusetts 02115, United States

Carlos E. Sanz-Rodriguez – Center for Tropical and Emerging Global Diseases, University of Georgia, Athens, Georgia 30602, United States; orcid.org/0000-0002-6759-1955

Courtney Fu – Department of Chemistry and Chemical Biology, Northeastern University, Boston, Massachusetts 02115, United States

Catherine LeBlanc – Department of Chemistry and Chemical Biology, Northeastern University, Boston, Massachusetts 02115, United States

Erin Burchfield – Department of Chemistry and Chemical Biology, Northeastern University, Boston, Massachusetts 02115, United States

Nyle Sharif – Department of Chemistry and Chemical Biology, Northeastern University, Boston, Massachusetts 02115, United States

Benjamin Hoffman – Center for Tropical and Emerging Global Diseases, University of Georgia, Athens, Georgia 30602, United States

Gaurav Kumar – Department of Molecular and Cellular Biology, Kennesaw State University, Kennesaw, Georgia 30144, United States

Andrei Purmal – Incuron Inc., Buffalo, New York 14203, United States

Complete contact information is available at:

<https://pubs.acs.org/doi/10.1021/acs.jmedchem.2c01767>

Notes

The authors declare no competing financial interest.

■ ACKNOWLEDGMENTS

The authors acknowledge Drs. Norma Roncal and Robert Campbell, Walter Reed Army Institute for Research, for performing the HepG2 toxicity assays and are grateful to AstraZeneca and Charles River Laboratories for the provision of *in vitro* ADME data in support of this project. The authors also acknowledge the National Institutes of Health for support of this work: R01AI124046 and R01AI126311.

■ ABBREVIATIONS USED

ACN, acetonitrile; ADME, absorption, distribution, metabolism, and excretion; AUC, area under the curve; Aq. sol., thermodynamic aqueous solubility; BINAP, 2,2'-bis-(diphenylphosphino)-1,1'-binaphthyl; CL_{int}, intrinsic clearance; CNS, central nervous system; DIPEA, *N,N*-diisopropylethylamine; DMF, dimethylformamide; HAT, human African trypanosomiasis; HLM, human liver microsomes; IPA, isopropyl alcohol; LLE, lipophilic ligand efficiency; NTDs, neglected tropical diseases; PK, pharmacokinetics; PPB, plasma protein binding; PSA, polar surface area; rMTD, repeated maximum tolerated dose; SAR, structure–activity relationship; SPR, structure–property relationship; TFA, trifluoroacetic acid

■ REFERENCES

- (1) NIH-NIAID. Neglected Tropical Diseases. <https://www.niaid.nih.gov/research/neglected-tropical-diseases> (accessed June 02, 2021). WHO. Trypanosomiasis, Human African (Sleeping Sickness). [https://www.who.int/news-room/fact-sheets/detail/trypanosomiasis-human-african-\(sleeping-sickness\)](https://www.who.int/news-room/fact-sheets/detail/trypanosomiasis-human-african-(sleeping-sickness)) (accessed June 2, 2021).
- (2) Singh, B.; Diaz-Gonzalez, R.; Ceballos-Perez, G.; Rojas-Barros, D. I.; Gunaganti, N.; Gillingwater, K.; Martinez-Martinez, M. S.; Manzano, P.; Navarro, M.; Pollastri, M. P. Medicinal Chemistry Optimization of a Diaminopurine Chemotype: Toward a Lead for *Trypanosoma brucei* Inhibitors. *J. Med. Chem.* **2020**, *63*, 9912–9927.
- (3) Thomas, S. M.; Purmal, A.; Pollastri, M.; Mensa-Wilmot, K. Discovery of a Carbazole-Derived Lead Drug for Human African Trypanosomiasis. *Sci. Rep.* **2016**, *6*, No. 32083.
- (4) Sarantopoulos, J. I. R.; Dowlati, A.; Ahluwalia, M. A Phase 1 Trial of CBL0137 in Patients With Metastatic or Unresectable Advanced Solid Neoplasm. *ClinicalTrials.gov Identifier*

- NCT01905228, 2020. <https://clinicaltrials.gov/ct2/show/NCT01905228> (accessed August 22, 2022). Ziegler, D. S. CBL0137 for the Treatment of Relapsed or Refractory Solid Tumors, Including CNS Tumors and Lymphoma. ClinicalTrials.gov Identifier NCT04870944, 2022. <https://clinicaltrials.gov/ct2/show/NCT04870944> (accessed October 22, 2022).
- (5) Gupta, M.; Lee, H. J.; Barden, C. J.; Weaver, D. F. The Blood-Brain Barrier (BBB) Score. *J. Med. Chem.* **2019**, *62*, 9824–9836.
- Wager, T. T.; Hou, X.; Verhoest, P. R.; Villalobos, A. Moving beyond rules: the development of a central nervous system multiparameter optimization (CNS MPO) approach to enable alignment of druglike properties. *ACS Chem. Neurosci.* **2010**, *1*, 435–449.
- (6) Tucker, J.; Sviridov, S.; Brodsky, L.; Burkhart, C.; Purmal, A.; Gurova, K.; Gudkov, A. Carbazole Compounds as p53 Activators and Their Preparation, Pharmaceutical Compositions and Use in the Treatment of Diseases. WO Patent WO20100424452010.
- (7) Hopkins, A. L.; Keseru, G. M.; Leeson, P. D.; Rees, D. C.; Reynolds, C. H. The role of ligand efficiency metrics in drug discovery. *Nat. Rev. Drug Discovery* **2014**, *13*, 105–121. Hughes, J. D.; Blagg, J.; Price, D. A.; Bailey, S.; Decrescenzo, G. A.; Devraj, R. V.; Ellsworth, E.; Fobian, Y. M.; Gibbs, M. E.; Gilles, R. W.; et al. Physicochemical drug properties associated with in vivo toxicological outcomes. *Bioorg. Med. Chem. Lett.* **2008**, *18*, 4872–4875.
- (8) Bachovchin, K. A.; Sharma, A.; Bag, S.; Klug, D. M.; Schneider, K. M.; Singh, B.; Jalani, H. B.; Buskes, M. J.; Mehta, N.; Tanghe, S.; et al. Improvement of Aqueous Solubility of Lapatinib-Derived Analogues: Identification of a Quinolinimine Lead for Human African Trypanosomiasis Drug Development. *J. Med. Chem.* **2019**, *62*, 665–687. Sanz-Rodríguez, C. E.; Hoffman, B.; Guyett, P. J.; Purmal, A.; Singh, B.; Pollastri, M.; Mensa-Wilmot, K. Physiologic Targets and Modes of Action for CBL0137, a Lead for Human African Trypanosomiasis Drug Development. *Mol. Pharmacol.* **2022**, *102*, 422–437.
- (9) Claes, F.; Vodnala, S. K.; van Reet, N.; Boucher, N.; Lunden-Miguel, H.; Baltz, T.; Goddeeris, B. M.; Buscher, P.; Rottenberg, M. E. Bioluminescent imaging of *Trypanosoma brucei* shows preferential testis dissemination which may hamper drug efficacy in sleeping sickness. *PLoS Neglected Trop. Dis.* **2009**, *3*, No. e486.
- (10) Faria, J.; Moraes, C. B.; Song, R.; Pascoalino, B. S.; Lee, N.; Siqueira-Neto, J. L.; Cruz, D. J.; Parkinson, T.; Ioset, J. R.; Cordeiro-da-Silva, A.; Freitas-Junior, L. H. Drug discovery for human African trypanosomiasis: identification of novel scaffolds by the newly developed HTS SYBR Green assay for *Trypanosoma brucei*. *J. Biomol. Screening* **2015**, *20*, 70–81.
- (11) Trindade, S.; Rijo-Ferreira, F.; Carvalho, T.; Pinto-Neves, D.; Guegan, F.; Aresta-Branco, F.; Bento, F.; Young, S. A.; Pinto, A.; Van Den Abbeele, J.; et al. *Trypanosoma brucei* Parasites Occupy and Functionally Adapt to the Adipose Tissue in Mice. *Cell Host Microbe* **2016**, *19*, 837–848.
- (12) Weseliński, Ł.; Luebke, R.; Eddaoudi, M. A Convenient Preparation of 9H-Carbazole-3,6-dicarbonitrile and 9H-Carbazole-3,6-dicarboxylic Acid. *Synthesis* **2014**, *46*, 596–599.
- (13) Ablá, N.; Bashyam, S.; Charman, S. A.; Greco, B.; Hewitt, P.; Jimenez-Diaz, M. B.; Katneni, K.; Kubas, H.; Picard, D.; Sambandan, Y.; et al. Long-Lasting and Fast-Acting in Vivo Efficacious Antiplasmodial Azepanylcarbazole Amino Alcohol. *ACS Med. Chem. Lett.* **2017**, *8*, 1304–1308.
- (14) Li, K.; Liu, M.; Yang, S.; Chen, Y.; He, Y.; Murtaza, I.; Goto, O.; Shen, C.; Meng, H.; He, G. Substitution effect of super hydrophobic units: A new strategy to design deep blue fluorescent emitters. *Dyes Pigm.* **2017**, *139*, 747–755.
- (15) Krause, S.; Evans, J. D.; Bon, V.; Senkovska, I.; Ehrling, S.; Stoek, U.; Yot, P. G.; Iacomini, P.; Llewellyn, P.; Maurin, G.; et al. Adsorption Contraction Mechanics: Understanding Breathing Energetics in Isorecticular Metal-Organic Frameworks. *J. Phys. Chem. C* **2018**, *122*, 19171–19179.
- (16) Ban, J.; Lim, M.; Shabbir, S.; Baek, J.; Rhee, H. Site-Specific Synthesis of Carbazole Derivatives through Aryl Homocoupling and Amination. *Synthesis* **2020**, *52*, 917–927.
- (17) McLatchie, A. P.; Burrell-Saward, H.; Myburgh, E.; Lewis, M. D.; Ward, T. H.; Mottram, J. C.; Croft, S. L.; Kelly, J. M.; Taylor, M. C. Highly sensitive in vivo imaging of *Trypanosoma brucei* expressing “red-shifted” luciferase. *PLoS Neglected Trop. Dis.* **2013**, *7*, No. e2571.